

Forecasting day-ahead electricity prices in Europe: the importance of considering market integration

Jesus Lago^{a,b,1}, Fjo De Ridder^b, Peter Vranx^c, Bart De Schutter^a

^a*Delft Center for Systems and Control, Delft University of Technology,
Mekelweg 2, 2628 Delft, The Netherlands*

^b*Energy Technology, VITO-Energyville, ThorPark, 3600 Genk, Belgium*

^c*AI Lab, Vrije Universiteit Brussel, Pleinlaan 2, 1050 Brussels, Belgium*

Abstract

Motivated by the increasing integration among electricity markets, in this paper we propose three different methods to incorporate market integration in electricity price forecasting and to improve the predictive performance. First, we propose a deep neural network that considers features from connected markets to improve the predictive accuracy in a local market. To measure the importance of these features, we propose a novel feature selection algorithm that, by using Bayesian optimization and functional analysis of variance, analyzes the effect of the features on the algorithm performance. In addition, using market integration, we propose a second model that, by simultaneously predicting prices from two markets, improves even further the forecasting accuracy. Finally, we present a third model to predict the probability of price spikes; then, we use it as an input in the other two forecasters to detect spikes. As a case study, we consider the electricity market in Belgium and the improvements in forecasting accuracy when using various French electricity features. In detail, we show that the three proposed models lead to improvements that are statistically significant. Particularly, due to market integration, predictive accuracy is improved from 15.7% to 12.5% sMAPE (symmetric mean absolute percentage error). In addition, we also show that the proposed feature selection algorithm is able to perform a correct assessment, i.e. to discard the irrelevant features.

Keywords: Electricity Price Forecasting, Electricity Market Integration, Deep Neural Networks, Functional ANOVA, Bayesian Optimization

1. Introduction

As a result of the liberalization and deregulation of the electricity markets in the last two decades, the dynamics of electricity trade have been completely reshaped. In particular, electricity has become a commodity that displays a set of characteristics that are uncommon to other markets: constant balance between production and consumption [1], load and generation influenced by external weather conditions, and dependence of the consumption on the hour of the day, day of the week, and time of the year [2]. Due to these facts, the dynamics of electricity prices exhibit behavior unseen in other markets, e.g. sudden and unexpected

price peaks or seasonality of prices at three different levels (daily, weekly and yearly) [2].

As a result of this unique behavior, electricity markets have become a central point of research in the energy sector and accurate electricity price forecasting has emerged as one of the biggest challenges faced by the different market entities. The usual motivation behind these efforts is a purely economic one; particularly, as forecasting accuracy increases, the negative economic effects of price uncertainty are mitigated and the market players make an economic profit. In addition, besides the economic point, another important fact to consider is that electricity markets are established to keep the grid stable. In particular, as prices become more volatile, the balance of the grid is compromised, strategic reserves have to be used, and the risk of a blackout increases. Therefore, by accu-

*Corresponding author

Email address: j.lagogarcia@tudelft.nl (Jesus Lago)

rately forecasting electricity prices, not only economic profit can be made, but also system stability is improved.

Due to the above motivations, electricity price forecasting has been continuously developed and improved for the last decades, and as a result, the literature comprises a large variety of distinctive approaches, e.g. see the literature reviews of [2, 3]. Nevertheless, to the best of our knowledge, a topic that has been not yet addressed is the influence of neighboring and connected markets into the forecast accuracy. In particular, as different areas in the world, e.g. the European Union [4], are enforcing a larger level of integration across national electricity markets, it is sensible to think that neighboring markets might play a role in the forecasting efficiency.

This paper focuses on addressing this scientific gap via two contributions: first, using a model that considers market integration, it analyzes the several improvements that can be achieved in forecasting accuracy when features from neighboring connected markets are taken into account; secondly, it also proposes a dual-market forecaster that, by simultaneously predicting the prices of two connected markets, uses market integration to further improve the predictive accuracy. As a case study, to test the proposed methods, the paper considers the price dynamics of the *European Power Exchange (EPEX)* in Belgium (EPEX-Belgium) and uses the features from the connected EPEX-France market to improve the predictive accuracy. In addition, while addressing the mentioned gap, the paper also enriches the scientific field with two extra contributions: a novel feature selection algorithm based on *Bayesian optimization* and *functional analysis of variance (fANOVA)*, and a model to predict the probability of price spikes in the day-ahead market.

1.1. Literature Survey

In this first introductory section, we present the literature review of three topics that are relevant for the research:

1. Electricity price forecasting.
2. Market integration.
3. Feature selection in electricity price forecasting.

1.1.1. Electricity Price Forecasting

It is important to note that the literature in the field of electricity price forecasting is quite substantial and that by no means we attempt to perform a

complete review of it. Instead, a concise overview is provided in order to be able to locate what are the state of the art techniques. To obtain a more extensive view of the state of the field, [2] provides a detailed review analyzing the research done in the last decades.

Basically, the price forecasting literature is typically divided in five areas: (1) multi-agent or game theory models simulating the operation of market agents, (2) fundamental methods employing physical and economic factors, (3) reduced-form models using statistical properties of electricity for risk and derivatives evaluation, (4) statistical models comprising time series and econometric models, and (5) artificial intelligence methods [2]. For forecasting day-ahead prices, or in general any other electricity spot prices, statistical and artificial intelligence methods have showed the best results [2]. As a result, they are the main focus of the review.

Typical statistical methods are: dynamic regression [5], AR and ARX models [6], ARIMA models [7, 8], transfer function [5], double seasonal Holt-Winter [9], TARX [10], semi/non-parametric models [6, 11], or GARCH-based models [12, 13]. In addition, within the same class of methods, different hybrid models have been also applied, e.g. wavelet-based models [7, 14].

Statistical models are usually linear forecasters, and as such, they are successful in the areas where the frequency of the data is low, e.g. weekly patterns. However, for hourly values, the nonlinear behavior of the data might be too complicated to predict [15]. As a result, motivated by the need for forecasters that are able to predict the nonlinear behaviors of hourly prices, several artificial intelligence methods have been proposed. Among these methods, Artificial Neural Networks [16, 17], Support Vector Regressors [18, 19], Radial Basis Function Networks [20, 21], or Fuzzy Networks [22] are among the most commonly used. In a recent study, [23] showed that *Deep Neural Networks (DNNs)* can also be a successful alternative.

The results comparing the accuracy of the mentioned models have produced unclear conclusions [17]. In general, the effectiveness of each model seems to depend on the market under study and on the period considered.

1.1.2. Market Integration

In the last decades, the EU has passed several laws trying to achieve a single and integrated European electricity market [4, 24]. At the moment,

while a single market is far from existing, there is evidence suggesting that the level of integration across the different regional markets has been increasing over time [25]. In particular, the evidence suggests that in the case of Belgium and France, the spot prices share strong common dynamics [26].

While some researchers have evaluated the level of integration of the European markets [25–27], and others have proposed statistical models to evaluate the probability of spike transmissions across EU markets [28], the literature regarding market integration to improve forecasting accuracy is rather scarce. In particular, to the best of our knowledge, only two other works have taken into account some sort of market integration, namely [29] and [30].

In detail, [29] analyzes the effect of using the day-ahead prices of the *Energy Exchange Austria (EXAA)* on a given day to forecast the prices of other European markets on the same day. In particular, using the fact that for the EXAA market the clearing prices are released before the closure of other European markets, [29] models the price dynamics of several European markets and considers the EXAA prices of the same day as part of these models. It is shown that, for certain European markets, using the available prices from the EXAA improves the forecasting accuracy in a statistically significant manner.

Similarly, [30] considers external price forecasts from other European markets as exogenous inputs of an artificial neural network to predict Italian day-ahead prices. Then, [30] shows that using the given forecasts the accuracy of their network can be improved from 19.08% to 18.40% *mean absolute percentage error (MAPE)*.

1.1.3. Feature Selection

Typically, three families of methods to perform feature selection exist: *filter*, *wrapper*, and *embedded methods* [31]. Filter methods apply some statistical measure in order to assess the importance of features. Their main disadvantage is that, as the specific model performance is not evaluated and the relations between features are not considered, they could select redundant information or avoid choosing some important features. Their main advantage is that, as a model does not have to be estimated, they are very fast. By contrast, wrapper methods perform a search across several feature sets, evaluating the performance of a given set by first estimating the prediction model and then using the predictive accuracy of the model as the performance

measure of the set. Their main advantage is that they consider a more realistic evaluation of the performance and interrelations of the features; their drawback is a long computation time. Finally, embedded methods, e.g. regularization [32, Chapter 7], learn the feature selection at the same time the model is estimated. Their advantage is that, while being less computationally expensive than wrapper methods, they still consider the underlying model. However, as a drawback, they are specific to a learning algorithm, and thus, they cannot always be applied.

Approaches for feature selection in the electricity price forecasting literature vary according to the prediction model used. For time series methods using only prices, e.g. ARIMA, autocorrelation plots (a filter method) [7, 8], or the Akaike information criterion (a wrapper method) [33] have been commonly used. In the case of forecasters with explanatory variables, e.g. neural networks, most researchers have used trial and error or filter methods based on linear analysis techniques: statistical sensitivity analysis [9, 16], correlation analysis [34], or principal component analysis [35]. Since prices display nonlinear dynamics, the mentioned techniques might be limited [36]; to solve that, different nonlinear filter methods such as the relief algorithm [37] or the mutual information technique [36, 38] have been proposed. More recently, a hybrid nonlinear filter-wrapper method, which uses mutual information and information content as a first filter step and a real-coded genetic algorithm as a second wrapper step, has been also proposed [39].

It is important to note that, while the algorithms proposed in the literature are fast decision-making techniques, they all consider a filter step where features are selected disregarding their effect on the accuracy of the prediction model. As a result, the resulting selected features might be, in some cases, redundant or incomplete.

1.2. Motivation and Contributions

While [29] and [30] have provided an initial assessment of possible forecasting improvements when considering market integration, there are still several gaps that have to be addressed. In particular, both works have only considered, as integration features, the prices in other markets during the same day that is being predicted; nevertheless, obtaining such information is limited to particular situations, and thus, the proposed models and improvements cannot be easily generalized. More

specifically, in the case of [29], the prices of the same day can be obtained because the EXAA releases its clearing prices earlier; nevertheless, that is not the case for other European markets. Similarly, [30] obtained the prices using some external forecasts; as a result, the improvements of considering integration depends on the source and accuracy of the forecasts used.

To overcome these limitations, in this paper we take a completely different approach and we use past prices from other markets as integration features. In addition, unlike the other studies, we also consider other market features in addition to prices; in particular, to enhance our models, we use day-ahead forecasts of the grid load and available generation in connected markets. As this type of information is widely available for other EU markets, the approach and proposed models should be easily generalizable to other markets. To perform the actual forecasting, we propose various models; particularly, considering the findings of [23], which shows that for the Belgian market and for recent years DNN structures are the best alternative, we propose a modeling framework with DNNs as building blocks.

Together with the described research, we also contribute to the literature of feature selection. In particular, we consider that, while the feature selection methods for electricity price forecasting proposed in the literature provide good and fast algorithms, they suffer from two main drawbacks:

1. They all perform a filter step where the model performance is not directly considered but a statistical measure is used instead.
2. In addition, in the case of nonlinear methods, the different inputs have to be transformed, e.g. in the mutual information technique [36] the inputs of a model are approximated by binomial variables. As a result, the selection is not done over the original feature set and some feature information might be lost.

To tackle these issues, we propose, as an additional contribution, a nonlinear wrapper feature selection algorithm that evaluates the feature performances on the prediction model and characterizes feature importance by means of functional ANOVA. While the approach is more computationally expensive than previously proposed methods, it can provide a more accurate assessment of the features. In particular, as it directly measures the feature performance on the real nonlinear model without per-

forming feature transformations, and as it takes into account feature interrelations, the algorithm is expected to be more accurate than current filter methods.

In summary, in this paper we analyze the effects of electricity market integration in forecasting accuracy and propose a set of models that take this effect into account to enhance the predictive performance. In particular, the main and most important contributions of this paper can be outlined as follows:

1. A forecasting model is developed which considers market integration by taking into account available features at day $d - 1$ in a neighboring market to improve the forecast accuracy of day-ahead prices at day d . Unlike previous works, the information used is widely available for most markets, making the prediction model a forecaster that can be generalized to other regions.
2. A second prediction model that also considers market integration is proposed. Specifically, by simultaneously predicting the day-ahead prices of two markets, the new model is able to model the effects of market integration even better and to improve the performance of the first proposed model.

In addition to the two main contributions, the paper also adds value to the scientific field by two additional contributions:

3. A novel feature selection algorithm is developed based on functional ANOVA, a tool that has been proposed to analyze the importance of mode hyperparameters [40].
4. A prediction model for price spike probability is also proposed. The model is used as an input for the two other proposed forecasters in order to enhance the predictive accuracy.

In order to analyze the performance of the proposed methods, a case study is considered. In particular, using data from the EPEX-Belgium and EPEX-France, the proposed models are shown to obtain improvements that are statistically significant and the feature selection algorithm is shown to select correct features.

The paper is organized as follows: Section 2 starts by introducing and explaining the different theoretical concepts that are used and modified in the research. Next, Section 3 proposes the modeling framework that considers market integration

in day-ahead price forecasting. Section 4 uses the theory of Section 2 to propose the novel approach to perform feature selection. Then, Section 5 starts the case study by describing and motivating the data used in the research; next, it selects the relevant features and illustrates the performance of the proposed feature selection algorithm. Finally, Section 6 evaluates the modeling framework by analyzing the statistical significance of the improvements on predictive accuracy obtained by the proposed models.

2. Theoretical background

In this section we first introduce the theoretical concepts and algorithms that are used and/or modified in the research. In particular, Section 2.1 briefly describes forecasting day-ahead prices. Then, Section 2.2 introduces DNNs, the chosen model for predicting prices. Section 2.3 presents hyperparameter optimization and analysis, foundations that are used for the novel feature selection algorithm. Then, Section 2.4 describes the metric used to assess the accuracy and performance of the proposed models. Finally, Section 2.5 defines the Diebold-Mariano test, a tool to assess the statistical significance of predictive accuracy.

2.1. Day-ahead Forecasting

The day-ahead electricity market is a type of power exchange widely used in several regions of the world. In its most general format, producers and consumers have to submit bids for the 24 hours of day d before some deadline on day $d-1$ (in most European markets, this deadline occurs at 11:00 or 12:00 am). Except for some markets, these bids are typically defined per hour, i.e. every market player has to submit 24 bids.

After the deadline, the market operator takes into account all the bids and computes the market clearing price for each of the 24 hours. Then, consumer/producer bids larger/lower or equal than the market clearing prices are approved, and a contract where the bids must be satisfied is established.

Based on the above facts, a useful forecaster of the day ahead market should be able to predict the set of 24 market clearing prices of day d based on the information available before the deadline of day $d-1$.

2.2. Deep Learning and DNNs

During the last decade, the field of neural networks has gone through some major innovations that have led to what nowadays is known as deep learning. Specifically, the term deep refers to the fact that, thanks to the novel developments of recent years, we can now train different neural network configurations whose depth is not just limited to a single hidden layer (as in the traditional multilayer perceptron), and which have systemically showed better generalization capabilities. As a result, in order to stress the importance of the depth in the achieved improvements, this new field of neural networks is now usually called deep learning [32].

While there are different DNN architectures, e.g. convolutional networks or recurrent networks, in this paper we consider a standard DNN, i.e. a multilayer perceptron with more than a single hidden layer.

2.2.1. Representation

Defining by $\mathbf{X} = [x_1, \dots, x_n]^\top \in \mathbb{R}^n$ the input of the network, by $\mathbf{Y} = [y_1, y_2, \dots, y_m]^\top \in \mathbb{R}^m$ the output of the network, by n_k the number of neurons of the k^{th} hidden layer, and by $\mathbf{z}_k = [z_{k1}, \dots, z_{kn_k}]^\top$ the state vector in the k^{th} hidden layer, a general DNN with two hidden layers can be represented by Figure 1.

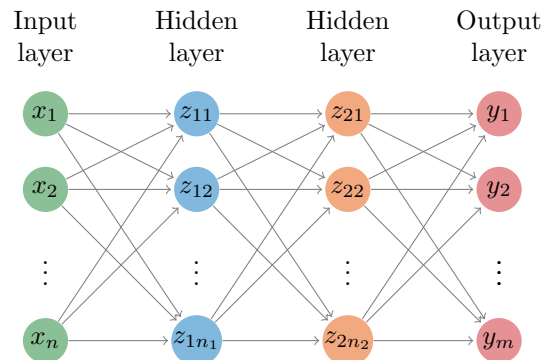


Figure 1: Example of a DNN.

2.2.2. Model Parameters

The parameters of a DNN are represented by a set of weights that establish the mapping connections between the different neurons of the network. In particular, in the most general case, the parameters could be defined as follows:

- $\mathbf{W}_{\text{in},i}$: the vector of weights between the input \mathbf{X} and the neuron i of the first hidden layer.
- \mathbf{W}_{ki} : the vector of weights from the $(k-1)^{\text{th}}$ hidden layer to neuron i in the k^{th} hidden layer.
- $\mathbf{W}_{o,i}$: the weights between the last hidden layer and output y_i .
- $\mathbf{b}_k = [b_{k1}, \dots, b_{knk}]^\top$: the vector of bias weights in the k^{th} hidden layer.
- $\mathbf{b}_o = [b_{o,1}, \dots, b_{o,m}]^\top$: the vector of bias weights in the output layer.

2.2.3. Model Equations

Based on the above definitions, the equations of a general DNN with l hidden layers can be defined by:

$$z_{1i} = f_{1i}(\mathbf{W}_{\text{in},i}^\top \cdot \mathbf{X} + b_{1i}), \quad \text{for } i = 1, \dots, n_1, \quad (1a)$$

$$z_{ki} = f_{ki}(\mathbf{W}_{ki}^\top \cdot \mathbf{z}_{k-1} + b_{ki}), \quad \text{for } i = 1, \dots, n_k, \quad (1b)$$

$$k = 2, \dots, l,$$

$$y_i = f_{o,i}(\mathbf{W}_{o,i}^\top \cdot \mathbf{z}_l + b_{o,i}), \quad \text{for } i = 1, \dots, m, \quad (1c)$$

where f_{ki} represents the activation function of neuron i in of the k^{th} hidden layer and $f_{o,i}$ the activation function of neuron i in the output layer. Typical activation functions are the sigmoid function, the hyperbolic tangent function, or the rectified linear unit.

2.2.4. Training

The process of estimating the model weights is usually called training. In particular, given a N -dimensional training set $\mathcal{S}_{\mathcal{T}} = \{(\mathbf{X}_k, \mathbf{Y}_k)\}_{k=1}^N$, the network training is done by solving a general optimization problem with the following structure:

$$\underset{\mathbf{W}}{\text{minimize}} \quad \sum_{k=1}^N g_k(\mathbf{Y}_k, F(\mathbf{X}_k, \mathbf{W})), \quad (2)$$

where \mathbf{W} is the vector concatenating all the network weights, $F: \mathbb{R}^n \rightarrow \mathbb{R}^m$ is the full neural network vectorial map, and g_k is the problem-specific cost function. Traditional methods to solve (2) include *gradient descent* or the *Levenberg–Marquardt* algorithm [2]. However, while these methods work well for small sized-networks, they display computational and scalability issues for DNNs. In particular, better alternatives for DNNs are the *stochastic gradient descent* [41] and all its variants [42];

in detail, by exploiting the fact that the objective function is a sum of functions g_k that only depend on the input sample $(\mathbf{X}_k, \mathbf{Y}_k)$, stochastic gradient descent computes approximations of the real gradient and provides a faster training algorithm that often obtains better results [43].

As a final remark, it is important to note that (2) is an approximation of the real problem we wish to minimize. Particularly, in an ideal situation, we would minimize the cost function w.r.t. to the underlying data distribution; however, as the distribution is unknown, the problem has to be approximated by minimizing the cost function over the finite training set. This is specially relevant for neural networks, where a model could overfit and have a good performance in the training set, but perform badly in the test set, i.e. a set with a different data distribution. To avoid this situation, the network is usually trained in combination with other techniques, e.g. regularization, early stopping and out-of-sample data to evaluate the performance.

2.2.5. Network Hyperparameters

In addition to the weights, the network has a different set of parameters that need to be selected before the training process. Typical parameters include the number of neurons of the hidden layers, the number of hidden layers, the type of activation functions, or the learning rate of the stochastic gradient descent method. To distinguish them from the main parameters, i.e. the network weights, they are referred to as the model hyperparameters.

2.3. Hyperparameter Selection

In order to perform the selection of the network hyperparameters, papers in the field of electricity price forecasting have traditionally defined a number of configurations and chosen the one with the best performance [9, 17, 30, 34, 36, 44]. Another approach, yet less usual, has been the use of evolutionary optimization algorithms in order to select the best network configuration [21]. However, while these approaches might work under some conditions, they have different flaws. In particular, while the first method implements fast decision-making, it does not provide an optimal selection of hyperparameters. Similarly, while the second method optimizes the selection, it evaluates a very large number of points in the hyperparameter space. As a result, if the function to be evaluated is costly, e.g. training a DNN, the second method requires large computation times.

An alternative to tackle these issues is *Bayesian optimization* [45], a family of algorithms for optimizing black-box functions that require a lower number of function evaluations than evolutionary optimization techniques. In detail, their working principle is to sequentially evaluate new samples in the function space, but drawing new samples by using the information obtained in the previously explored samples as a prior belief. Based on that, they reduce the number of evaluated sample points and lead to a more efficient optimization.

2.3.1. Hyperparameter Optimization

Considering that the training of a DNN model is very costly, we take a different approach for the hyperparameter selection and consider a Bayesian optimization algorithm that has been widely used in the machine learning community. In particular, we use the *Tree-Structured Parzen Estimator (TPE)* [46], an optimization algorithm within the family of *sequential model-based optimization* methods [47]. The basic principle of a sequential model-based optimization algorithm is to optimize a black-box function, e.g. the performance of a neural network as a function of the hyperparameters, by iteratively estimating an approximation of the function and exploring the function space using the local minima of the approximation. In detail, at any given iteration i , the algorithm evaluates the black-box function at a new point θ_i . Next, it estimates an approximation \mathcal{M} of the black-box function by fitting the previously sampled points to the obtained function evaluations. Then, it selects the next sample point θ_{i+1} by numerically optimizing \mathcal{M} and starts the next iteration. Finally, after a maximum number of iterations T have been performed, the algorithm selects the best configuration.

In the case of a neural network and its hyperparameters, the algorithm evaluates the performance of a hyperparameter instantiation θ_i by training the neural network and computing its predictive accuracy p_i . Then, it estimates a model \mathcal{M} that fits all the past hyperparameter instantiations θ_i to the respective performances p_i , and selects the next instantiation θ_{i+1} by numerically optimizing \mathcal{M} . Algorithm 1 represents an example of a sequential model-based optimization algorithm for hyperparameter selection.

2.3.2. Hyperparameter Analysis

An optional step after hyperparameter optimization is to perform an analysis of the hyperparameter

Algorithm 1 Hyperparameter Optimization

```

1: procedure SMBO( $T, \theta_0$ )
2:    $\theta_i \leftarrow \theta_0$ 
3:    $\mathcal{H} \leftarrow \emptyset$ 
4:   for  $i = 1, \dots, T$  do
5:      $p_i \leftarrow \text{TrainNetwork}(\theta_i)$ 
6:      $\mathcal{H} \leftarrow \mathcal{H} \cup \{(p_i, \theta_i)\}$ 
7:     if  $i < T$  then
8:        $\mathcal{M}_i(\theta) \leftarrow \text{EstimateModel}(\mathcal{H})$ 
9:        $\theta_i \leftarrow \text{argmax}_{\theta} \mathcal{M}_i(\theta)$ 
10:    end if
11:  end for
12:   $\theta^* \leftarrow \text{BestHyperparameters}(\mathcal{H})$ 
13:  return  $\theta^*$ 
14: end procedure

```

importance. In particular, while the optimal hyperparameter configuration has been already obtained, it is unknown how much each hyperparameter contributes to the overall performance.

This type of study is specially relevant in order to avoid unnecessary model complexities; e.g. while the optimal number of neurons might be large, reducing the number of neurons might barely affect the performance. In that case, it might be better to use a smaller network and improve the algorithm computational speed at the cost of a slightly lower performance.

Functional ANOVA

An approach for carrying on such an analysis is proposed in [40], where a novel method based on random forests [48] and functional ANOVA is introduced. In particular, [40] considers the generic case of having n hyperparameters with domains $\Theta_1, \dots, \Theta_n$, and defines the following concepts:

- Hyperparameter set $N = \{1, \dots, n\}$.
- Hyperparameter space $\Theta : \Theta_1 \times \dots \times \Theta_n$.
- Hyperparameter instantiation $\theta = [\theta_1, \dots, \theta_n]^\top$.
- Hyperparameter subset $U = \{u_1, \dots, u_q\} \subseteq N$ and associated partial hyperparameter instantiation $\theta_U = [\theta_{u_1}, \dots, \theta_{u_q}]^\top$.

Then, given a set $\mathcal{H} = \{(\theta_k, p_k)\}_{k=1}^T$ of hyperparameter realizations, the proposed method fits a random forest model $\mathcal{M}_{\text{RF}}(\theta)$ to build a predictor

of the performance p as a function of the hyperparameter vector θ .

Then, using \mathcal{M}_{RF} , the method defines a *marginal performance predictor* $\hat{a}(\theta_U)$ as a forecaster of the performance of any partial hyperparameter instantiation θ_U . In particular, given a subset $U \subseteq N$, $\hat{a}(\theta_U)$ provides an estimation of the average performance across the hyperparameter space $N \setminus U$ when the hyperparameters of U are fixed at θ_U .

Finally, using the marginal performance predictor $\hat{a}(\theta_U)$, the algorithm carries out a functional ANOVA analysis to estimate the importance of each hyperparameter. In particular, defining the total variance across the performance by \mathbb{V} , the algorithm divides this quantity as a sum of individual contributions of different subsets $U \subseteq N$:

$$\mathbb{V} = \sum_{U \subseteq N} \mathbb{V}_U, \quad (3)$$

and then, the importance \mathbb{F}_U of each subset U is computed based on the subset contribution to the performance variance:

$$\mathbb{F}_U = \frac{\mathbb{V}_U}{\mathbb{V}}. \quad (4)$$

For the particular case of the hyperparameter importance, the algorithm just evaluates \mathbb{F}_U for each subset $U = \{i\}$ composed of a single hyperparameter. As in [40], we refer to the variance contributions \mathbb{F}_U of single hyperparameters as *main effects* and to the rest as *interaction effects*.

It is important to note that, in addition to the importance \mathbb{F}_U , the algorithm also provides, for each partial hyperparameter instantiation θ_U , the prediction of the marginal performance $\hat{a}(\theta_U)$ and an estimation of its standard deviation σ_{θ_U} .

2.4. Performance Metrics

In order to evaluate the accuracy of the proposed models, we need a performance metric. In this paper, as motivated below, we use the *symmetric mean absolute percentage error (sMAPE)* [49]. In particular, given a vector $\mathbf{Y} = [y_1, \dots, y_N]^\top$ of real outputs and a vector $\hat{\mathbf{Y}} = [\hat{y}_1, \dots, \hat{y}_N]^\top$ of predicted outputs, the sMAPE metric can be computed as:

$$\text{sMAPE} = \frac{100}{N} \sum_{k=1}^N \frac{|y_k - \hat{y}_k|}{(|y_k| + |\hat{y}_k|)/2}. \quad (5)$$

The reason for selecting the sMAPE instead of the more traditional MAPE is the fact that the MAPE

is affected by different issues [49]. Particularly, for our application, the MAPE becomes sensitive to values close to zero; in detail, when an output y_i gets close to zero, the corresponding MAPE contribution becomes very large and it dominates the final value.

2.5. Diebold-Mariano (DM) Test

The sMAPE metric defined above only provides an assessment on which model has, for the data use, a better accuracy. In particular, while the accuracy of a model can be higher, the difference in performance might be not significant enough to establish that the model is really better. Therefore, to assess the statistical significance in the difference of predictive accuracy performance, a commonly used tool is the Diebold-Mariano test [50].

In detail, given a time series vector $\mathbf{Y} = [y_1, \dots, y_N]^\top$ to be forecasted, two prediction models M_1 and M_2 , and the associated forecasting errors $\boldsymbol{\varepsilon}^{M_1} = [\varepsilon_1^{M_1}, \dots, \varepsilon_N^{M_1}]^\top$ and $\boldsymbol{\varepsilon}^{M_2} = [\varepsilon_1^{M_2}, \dots, \varepsilon_N^{M_2}]^\top$, the DM test evaluates whether there is a significant difference in performance accuracy based on an error loss function $L(\varepsilon_k^{M_i})$. In particular, the DM test builds a loss differential function as:

$$d_k^{M_1, M_2} = L(\varepsilon_k^{M_1}) - L(\varepsilon_k^{M_2}), \quad (6)$$

and then, it tests the null hypothesis H_0 of both models having equal accuracy, i.e. equal expected loss $\mathbb{E}(d_k^{M_1, M_2}) = 0$, against the alternative hypothesis H_1 of the models having different accuracy, i.e.:

$$\begin{array}{l} \text{Two-sided} \\ \text{DM test} \end{array} \left\{ \begin{array}{l} H_0 : \mathbb{E}(d_k^{M_1, M_2}) = 0, \\ H_1 : \mathbb{E}(d_k^{M_1, M_2}) \neq 0, \end{array} \right. \quad (7)$$

with \mathbb{E} representing the expected value. Similar to the standard two-sided test, a one-sided DM test can be built by testing the null hypothesis that the accuracy of M_1 is equal or worse than the accuracy of M_2 versus the alternative hypothesis of the accuracy of M_1 being better:

$$\begin{array}{l} \text{One-sided} \\ \text{DM test} \end{array} \left\{ \begin{array}{l} H_0 : \mathbb{E}(d_k^{M_1, M_2}) \geq 0, \\ H_1 : \mathbb{E}(d_k^{M_1, M_2}) < 0. \end{array} \right. \quad (8)$$

While the loss function L can be freely chosen, it has to ensure that the resulting loss differential is covariance stationary. A loss function that is typically used is:

$$L(\varepsilon_k^{M_i}) = |\varepsilon_k^{M_i}|^p, \quad (9)$$

where usually $p \in \{1, 2\}$.

3. Modeling Framework: Day-Ahead Forecasters with Market Integration

In this section, three different models are proposed to include market integration in day-ahead forecasting. While the three models integrate features from neighboring connected markets, the idea behind each one of them is different.

The first two models are similar to each other as both of them try to forecast the full set of day-ahead prices. However, they differ from each other in the number and type of prices that they predict; in particular, while the first model predicts the day-ahead prices of a single market, the second model combines a dual market prediction into a single model. The third model is completely different from the other two as, instead of forecasting prices, it tries to predict the probability of a price spike in the day-ahead market. The main idea is that, by detecting anomalies, the forecasting accuracy can be further improved.

3.1. Single-Market Day-Ahead Forecaster

The basic model for predicting day-ahead prices uses a DNN in order to forecast the set of 24 day-ahead prices.

3.1.1. DNN Model

Based on the results of [23], we select a DNN with two hidden layers as forecasting model. In particular, defining the input of the model as the relevant data $\mathbf{X} = [x_1, \dots, x_n]^\top \in \mathbb{R}^n$ available at day $d-1$ in the local and neighboring markets, and letting n_1 and n_2 be the number of neurons of the first and the second hidden layer respectively, and $\mathbf{p} = [p_1, p_2, \dots, p_{24}]^\top \in \mathbb{R}^{24}$ the set of 24 day-ahead prices to be forecasted, the proposed model can be represented by Figure 2. In addition, the equations of the model are given by (1), where in our case the number of hidden layers is $l = 2$ and the output dimension is $m = 24$.

3.1.2. Model Implementation Details

The DNN is trained by minimizing the mean absolute error. In particular, given the N -dimensional training set $\mathcal{S}_{\mathcal{T}} = \{(\mathbf{X}_k, \mathbf{p}_k)\}_{k=1}^N$, the optimization problem that is solved to train the neural network is:

$$\underset{\mathbf{W}}{\text{minimize}} \quad \sum_{k=1}^N \|\mathbf{p}_k - F(\mathbf{X}_k, \mathbf{W})\|_1, \quad (10)$$

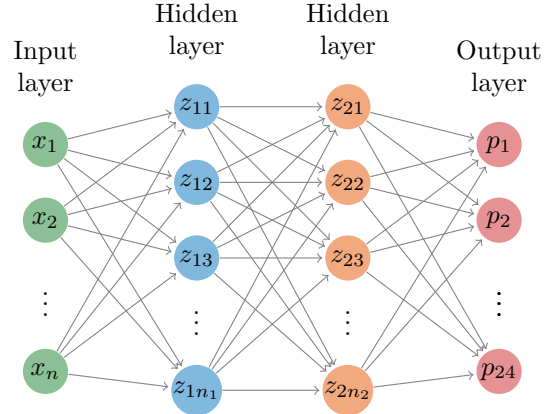


Figure 2: DNN to forecast day-ahead prices.

where, as in Section 2.2, \mathbf{W} represents the vector of all network weights and $F : \mathbb{R}^n \rightarrow \mathbb{R}^{24}$ is the neural network vectorial map. The selection of the mean absolute error instead of the more traditional root mean square error is done for a simple reason: as the electricity prices have very large spikes, the Euclidean norm would put too much importance on the spiky prices.

The optimization problem is initialized via single-start with the Glorot initialization [51] and solved using Adam [52], a version of the stochastic gradient descent method that computes adaptive learning rates for each model parameter. The selection of Adam is also done for a clear reason: as the learning rate is automatically computed by Adam, the time spent on tuning the optimizer is reduced. Together with Adam, the forecaster also considers early stopping [53] to avoid overfitting.

In addition, the rectified linear unit [54] is selected as the activation function of the hidden layers. However, as the prices are real numbers, no activation function is used for the output layer; instead, the following affine map is considered:

$$p_{B_i} = \mathbf{W}_{o_i}^\top \cdot \mathbf{h}_2 + b_{o_i}, \quad \text{for } i = 1, \dots, 24. \quad (11)$$

Finally, to select the dimension n of the network input and the dimensions n_1 and n_2 of the hidden layers, a feature selection and hyperparameter optimization are performed. In particular, both concepts are further explained in Section 4.

3.2. Dual Market Day-Ahead Forecaster

A possible variant of the single-market model is a forecaster that predicts the prices of two markets

in a single model. While this might seem counter-intuitive at first, i.e. adding extra outputs to the model could compromise its ability to forecast the set of 24 prices that we are really interested in, this approach can, in fact, lead to neural networks that are able to generalize better.

The general idea behind forecasting two markets together is that, as we expect prices in both markets to be interrelated and to have similar dynamics, by forecasting both time series in a single model we expect the neural network to learn more accurate relations and to generalize better. In particular, it has been empirically shown that DNNs can learn features that can, to some extent, generalize across tasks [55]. Similarly, it has also been shown that, by forcing DNNs to learn auxiliary related tasks, the performance and learning speed can be improved [56–58].

In more detail, there are some possible hypotheses that can explain why training with multiple outputs can help to improve the performance:

1. The simplest explanation is the amount of data: as more data is available, the neural network can learn more relevant features. Moreover, as the tasks are related, the neural network has more data to learn features that are common to all tasks.
2. A second reason is regularization: by solving different tasks, the network is forced to learn features useful for all tasks and to not overfit to the data of a single task.

In short, DNNs predicting multiple tasks can use more data and can learn more complex relations. Their only requirement is to employ auxiliary tasks that are sufficiently related to the main one so that the network can learn relevant features. However, it is important to keep in mind that these properties have only been confirmed empirically; therefore, how much multitasking can help depends on the specific problem; particularly, there might be cases where a single-task network could do better.

3.2.1. Model Implementation

Consider an electricity market B and a second electricity market F that is connected to B. Then, defining the output of the network by $\mathbf{p} = [p_{B_1}, \dots, p_{B_{24}}, p_{F_1}, \dots, p_{F_{24}}]^\top \in \mathbb{R}^{48}$, i.e. the set of 48 day-ahead prices from the market B and the market F, and keeping the rest of the DNN parameter definitions the same, the new DNN structure can

be represented by Figure 3. In addition, as both models only differ in the output size, the implementation details are exactly the same as defined for the single-market model in Section 3.1.2.

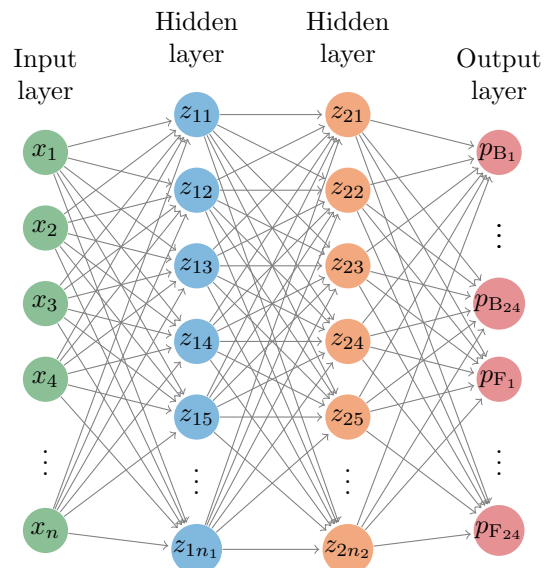


Figure 3: DNN to simultaneously forecast day-ahead prices in two markets.

3.3. Spike Probability Prediction

The dynamics of the electricity spot markets are known to display a mean-reverting behavior and very large, but sporadic, reverting price changes [59]. These extreme events are usually referred to as spikes, and they are almost an exclusive feature of electricity spot prices [2, 28].

In the case of Europe, spikes across spot markets seem to be partially dependent, e.g. the French market cospikes with the German, Dutch, and UK markets [28]. As a result, it seems necessary that, when modeling the dependency between French and Belgian markets, the forecaster should take into account the spikes. However, as the frequency of the spikes is rather low, when any prediction model is estimated, it is likely that the spikes would be left unconsidered. To avoid that, we propose a third model that outputs the probability of spikes for the 24 day-ahead prices and then uses them as inputs for the main forecasters.

3.3.1. Spikes: Mathematical Definition

The first step to build such a model is to provide a mathematical definition of a spike. In particular, we

regard a price to be a spike if, considering the interval comprising two weeks before and after the price, the price is not within the interval defined by the mean \pm three standard deviations; i.e. given a time series vector of prices $\mathbf{p} = [p_1, \dots, p_N]^\top$, the correspondent spike time series vector $\mathbf{s} = [s_1, \dots, s_N]^\top$ is built as:

$$s_k = \begin{cases} 0 & \text{if } p_k \in [\mu_k - 3\sigma_k, \mu_k + 3\sigma_k] \\ 1 & \text{otherwise} \end{cases}, \quad (12a)$$

where:

$$\mu_k = \text{mean}(p_{k-14 \times 24}, \dots, p_{k+14 \times 24}), \quad (12b)$$

$$\sigma_k = \text{std}(p_{k-14 \times 24}, \dots, p_{k+14 \times 24}). \quad (12c)$$

In order to have a better understanding of a definition of an outlier, Figure 4 depicts the prices in the EPEX-Belgium during 2015. The dashed lines define the intervals of $\mu_k \pm 3\sigma_k$, and thus, values below or above them represent the corresponding spikes. As can be seen, most of the prices are within the limits and the spikes are infrequent events.

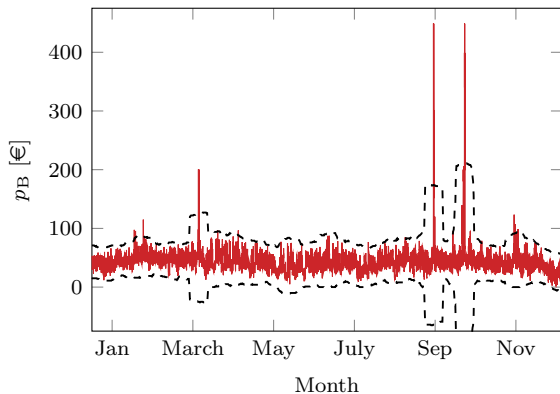


Figure 4: EPEX-Belgium prices in 2015. Dashed lines represent values above and below three times the standard deviation.

3.3.2. Predictive Model

In order to forecast the spike probability, we consider a similar DNN as used to model the previous two forecasters. Specifically, defining the vector of outliers to be forecasted by $\mathbf{s} = [s_1, \dots, s_{24}]^\top \in \mathbb{R}^{24}$, and keeping the same nomenclature as in Sections 3.1-3.2, the model can be represented by Figure 5.

3.3.3. Implementation Details

While the structure of this network is similar to the previous models, the implementation is different. Particularly, unlike the previous networks, the

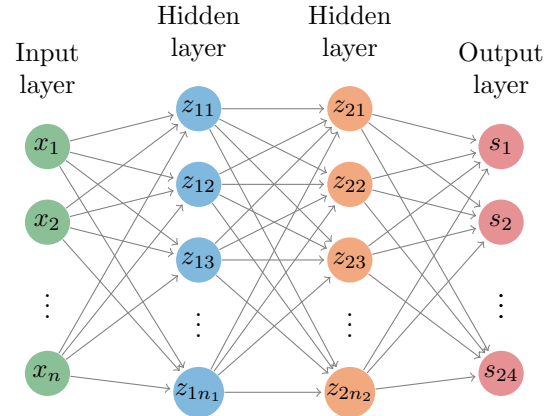


Figure 5: DNN to forecast probability of a spike on the day-ahead prices.

new model uses an activation function in the output layer; specifically, using the same nomenclature as before, the equations of the output layer are given by:

$$s_i = \text{sigmoid}(\mathbf{W}_{o_i}^\top \cdot \mathbf{z}_2 + b_{o_i}), \quad \text{for } i = 1, \dots, 24, \quad (13)$$

where, by using the sigmoid function, the spike s_i is able to model a probability, i.e. $s_i \in [0, 1]$.

A second difference in the implementation is the optimization problem that is solved to train the network. In particular, as the spike detection is a binary classification problem, the optimization problem minimizes the cross-entropy loss between the real and the predicted probability of an outlier:

$$\begin{aligned} \underset{\mathbf{W}}{\text{minimize}} \quad & \frac{1}{24N} \sum_{k=1}^N \left(\mu (F(\mathbf{X}_k, \mathbf{W}))^\top \log(\mathbf{s}_k) + \right. \\ & \left. (1 - F(\mathbf{X}_k, \mathbf{W}))^\top \log(1 - \mathbf{s}_k) \right). \end{aligned} \quad (14)$$

As before, $\mathcal{S}_{\mathcal{T}} = \{(\mathbf{X}_k, \mathbf{s}_k)\}_{k=1}^N$ is the training dataset, \mathbf{W} the network weights, F the network map, and $\log(\mathbf{s}_k)$ is the element-wise log function on vector \mathbf{s}_k . In addition, the new model also has to use an extra parameter μ to account for the data imbalance [60]. In particular, as the spikes are rare events, the ratio of spikes to non-spikes is in the order of 1:1000. As a result, if nothing is done, the effect of spikes in the loss function is minimal and the training process disregards the spikes. To avoid that, we introduce μ to penalize negative misclassification errors (missing a spike) more and to

increase the importance of spikes in the loss function.

Despite the described differences, the other implementation details remain unchanged: the model is trained using Adam with early stopping and the activation functions of the hidden layers are again rectified linear units.

4. Feature Selection Algorithm

As explained in the introduction, while the feature selection methods for electricity price forecasting proposed in the literature provide good and fast algorithms, they have two drawbacks:

1. They perform a filter step where the model performance is not considered.
2. For the nonlinear methods, the different inputs have to be transformed, i.e. the selection is not done over the original feature set, and thus, some feature information might be lost.

Therefore, we propose a nonlinear wrapper method that directly evaluates the features on the prediction model; in particular, while the approach is more computationally demanding, it can provide a better selection as it uses the real predictive performance without any data transformations. In detail, in Section 2.3 we have introduced the TPE algorithm, a method for hyperparameter optimization, together with functional ANOVA, an approach for assessing hyperparameter importance. In this section, we combine both methods to build a feature selection algorithm that consists of four different steps:

1. Model the features as hyperparameters.
2. Optimize the hyperparameters/features.
3. Analyze the results.
4. Select the important features.

4.1. Features as Hyperparameters

The first step of the algorithm is to model the selection of features as model hyperparameters. In particular, we consider two types of features:

1. Binary features θ_B , whose selection can be done through a binary variable, i.e.

$$\theta_B \in \{0, 1\}, \quad (15)$$

where $\theta_B = 0$ would represent feature exclusion and $\theta_B = 1$ feature inclusion. They represent the type of features considered by traditional algorithms. An example would be

whether to include holidays data or whether to choose a specific lag in an ARIMA model.

2. Integer features θ_I , which not only can model the inclusion-exclusion of an input, but also select some associated size or length, i.e.

$$\theta_I \in \mathbb{Z}, \quad (16)$$

where $\theta_I = 0$ represents exclusion. Examples would be the number of past days of price data or the maximum lag of an ARIMA model.

Given these definitions, the binary features are modeled as hyperparameters using the hyperparameter space Θ_B and the hyperparameter set $B = \{1, \dots, n_B\}$. Likewise, the integer features are modeled by the hyperparameter space Θ_I and the hyperparameter set $I = \{1, \dots, n_I\}$. Finally, the full hyperparameter space is defined by $\Theta = \Theta_B \cup \Theta_I$ and the hyperparameter set by $N = B \cup I$.

4.2. Feature Optimization

The second step of the algorithm is to perform a TPE optimization over the hyperparameter-feature space. The result of the algorithm is the optimal feature selection θ^* together with the set $\mathcal{H} = \{(\theta_k, p_k)\}_{k=1}^T$ of feature-performance pairs, where p_k represents the model predictive accuracy when using the feature selection θ_k .

In a simpler version of the algorithm, the optimal feature selection would be represented by θ^* and the method could conclude here. Nevertheless, the fact that a feature is part of θ^* , does not guarantee that the feature is relevant; specifically, a feature might have little or no effect in the performance, and still, as long as it does not have a negative effect, it might appear in the optimal configuration. As a result, if no further processing is considered, the algorithm might select redundant features, and in turn, lead to more computationally expensive models and increase the risk of overfit.

4.3. Feature Analysis

To solve the problem of detecting unnecessary features, the algorithm comprises a third step where feature importance is analyzed. In particular, using the functional ANOVA methodology proposed by [40], the algorithm analyzes \mathcal{H} and provides the importance of each feature i and each pairwise interaction $\{i, j\}$ as the percentage-wise contribution to the performance variance \mathbb{V} . In detail, using the definitions given in Section 2.3.2 and (3)-(4), the

algorithm computes the importance of feature Θ_i and each pairwise interaction $\Theta_i \times \Theta_j$ by:

$$\mathbb{F}_{\{i\}} = \frac{\mathbb{V}_{\{i\}}}{\mathbb{V}}, \quad \mathbb{F}_{\{i,j\}} = \frac{\mathbb{V}_{\{i,j\}}}{\mathbb{V}}. \quad (17)$$

In addition, for each feature $i \in N$ and feature instantiation $\theta_i \in \Theta_i$, the algorithm also provides the predicted marginal performance $\hat{a}(\theta_i)$.

4.4. Feature Selection Algorithm

The fourth and final algorithm step is the selection itself. In particular, making use of the obtained $\mathbb{F}_{\{i\}}$, $\mathbb{F}_{\{i,j\}}$ and $\hat{a}(\theta_i)$, the selection procedure performs the following steps:

1. Define a threshold parameter $\epsilon \in (0, 1]$.
2. Make a pre-selection by discarding features that do not improve nor decrease the performance. In particular, regard features i whose importance $F_{\{i\}}$ is larger than ϵ :

$$U_1^* = \{i \in N \mid F_{\{i\}} > \epsilon\}, \quad (18a)$$

or features i which have at least one pairwise contribution $F_{\{i,j\}}$ larger than ϵ :

$$U_2^* = \{i \in N \mid \exists j \in N \setminus \{i\} : F_{\{i,j\}} > \epsilon\}. \quad (18b)$$

3. With the remaining features in $U_1^* \cup U_2^*$, perform a second selection U^* by discarding those whose predicted marginal performance $\hat{a}(\theta_i)$ is lower when being included than when being excluded, i.e.:

$$U^* = \{i \in U_1^* \cup U_2^* \mid \exists \theta_i \in \Theta_i : \mu_{\theta_{i,0}} < \hat{a}(\theta_i)\}, \quad (18c)$$

where $\mu_{\theta_{i,0}}$ represents the marginal performance $\hat{a}(\theta_i = 0)$ of excluding feature i .

4. Finally, the set of selected binary features can be obtained by:

$$U_B^* = U^* \cap B. \quad (18d)$$

Similarly, for the set of optimal integer features U_I^* , the selection is done in terms of the feature itself and the instantiation with the best performance:

$$U_I^* = \{\{i, \theta_i^*\} \mid i \in U^* \cap I, \theta_i^* = \operatorname{argmax}_{\theta_i} \hat{a}(\theta_i)\}. \quad (18e)$$

4.5. Discussion

It is important to note that, as the functional ANOVA algorithm requires independence of hyperparameters, conditional feature selection is not possible. In addition, it is also necessary to point out that we have used here functional ANOVA as a tool to obtain the required $\mathbb{F}_{\{i\}}$, $\mathbb{F}_{\{i,j\}}$, and $\hat{a}(\theta_i)$. As a consequence, the description given in this section and in Section 2.3.2 is very brief; for a more detailed explanation, [40] derives the full and original algorithm and should serve as a reference.

5. Case Study - Part I: Data and Model Selection

In order to assess the performance of the various models and algorithms, we consider, as a case study, the day-ahead prices in the EPEX-Belgium and the role that play the various features from the EPEX-France. For the sake of clearness, the case study is divided in two sections:

1. Section 5, where, as initial step in the study, the data, features and model hyperparameters are selected.
2. Section 6, where the predictive accuracy of the modeling framework with market integration is analyzed via hypothesis testing.

To perform the first step, this section is organized as follows: Section 5.1 introduces and motivates the choice of data for the case study. Next, in Section 5.2, the feature selection algorithm is applied in combination with a hyperparameter optimization; based on the results, the performance of the proposed algorithm is analyzed and the features for the proposed day-ahead forecasters are selected. Finally, Section 5.3 ends with a general discussion on the algorithm results and performance.

Before continuing with the case study, it is important to note that all the deep learning models used in this section and Section 6 are modeled using the same software: the Keras [61] deep learning library in combination with the mathematical modeling language Theano [62]. In addition, to speed up the computation time, all the models are trained using a GPU GeForce GTX 980.

5.1. Data

In this section, the data used for the research is introduced. Particularly, we motivate the reason of its selection, we describe the processing of the

data, and we explain how the data is divided into a training, validation and test sets in order to conduct the different experiments.

5.1.1. Data Selection and Motivation

In general, when looking at the day-ahead forecasting literature, many inputs have been proposed as meaningful explanatory variables, e.g. temperature, gas and coal prices, grid load, available generation or weather [2].

To make our selection, we try to make sure that the selected data is not only related to the price dynamics, but also fulfills some minimum requirements so that the proposed models can easily be exported to other European markets. Specifically, we only choose data that is freely available online for most EU markets. In particular, we select the period from 01/01/2010 to 31/11/2016 as the time range of study, and we consider the following data:

1. Day-ahead prices from the EPEX-Belgium and EPEX-France power exchanges. They are respectively denoted as p_B and p_F .
2. Day-ahead forecasts of the grid load and generation capacity in Belgium and France. Like in other European markets, these forecasts are available before the bid deadline on the website of the *transmission system operators (TSOs)*: ELIA for Belgium and RTE for France. They are respectively denoted as l_B and g_B for Belgium, and as l_F and g_F for France.
3. Calendar of holidays H_F and H_B in France and Belgium in the defined time range.

While it could be argued that different weather data could also be easily accessible and important for the forecasting, for our research, we have decided to disregard them for mainly three reasons:

1. Weather factors are already indirectly taken into account in the grid load and generation forecasts provided by the TSO. In particular, the generation forecast has to consider weather information regarding wind speed and solar radiation. Likewise, load forecasts also need to consider temperature and other weather variables to obtain the electricity consumption.
2. Moreover, weather data are local phenomena, and as such, they can greatly vary from one part of a country to another. As a result, unlike the grid load or generation data, it is not possible to select a single value of temperature or any other weather data for a given time interval.

5.1.2. Data Processing

An important thing to note is that the data used is mostly unprocessed. In particular, as we intend to forecast and detect spikes, price outliers are not eliminated. The only data transformation is a price interpolation and elimination every year corresponding respectively with the missing and extra values due to the daylight saving. In addition, while all the metrics and tests are computed using the real prices, the training of the neural networks is done with data normalized to the interval $[-1, 1]$. This last step is necessary because the input features have very different ranges; therefore, if the data is not normalized, the training time increases and the final result is a network that displays, in general, worse performance [43].

5.1.3. Data Division

To perform the different experiments, we divide the data into three sets:

1. Training set (01/01/2010 to 31/11/2014): these data are used for training and estimating the different models.
2. Validation set (01/11/2014 to 31/11/2015): a year of data is used to verify that the model does not overfit, i.e. performs early stopping, as well as to select optimal hyperparameters and features.
3. Test set (01/11/2015 to 31/11/2016): a year of data, which is not used at any step during the model estimation process, is employed as the out-of-sample dataset to compare and evaluate the models.

5.1.4. Data Access

For the sake of reproducibility, we have only used publicly available data. In particular, the load and generation day-ahead forecasts are available on the webpages of RTE [63] and Elia [64], the respective TSOs in France and Belgium. In the case of the prices, they can be obtained from the ENTSO-E transparency platform [65]. For the holidays, the dates are easily accessible with an internet search.¹

¹CONFIDENTIAL - To easily reproduce results during the review process and to facilitate the work of the reviewers, the data used is temporarily uploaded in www.google.com/kJk9Ec.

5.2. Feature Selection

In order to illustrate the proposed algorithm for feature selection, we use it to select the important features for predicting Belgian prices as well as to perform a first assessment of the effect of French data on the forecasting accuracy. Moreover, to perform the analysis, we consider the first and simpler DNN proposed in Section 3, i.e. the forecaster including inputs from two connected markets but predicting prices from a single market.

5.2.1. Feature Definition

In order to perform the feature selection, we first need to model each possible input as either a binary or an integer feature. As described in Section 5.1, the available features are the day ahead prices p_B and p_F , the day-ahead forecasts l_B and l_F of the grid load, the day-ahead forecasts g_B and g_F of the available generation, and the calendar of holidays H_B and H_F .

Considering that, given the market at time h , we aim at forecasting the time series vector $\mathbf{p}_{B,h} = [p_{B,h+1}, \dots, p_{B,h+24}]^\top$ of Belgian day-ahead prices, the use of the day-ahead loads $\mathbf{l}_{B,h} = [l_{B,h+1}, \dots, l_{B,h+24}]^\top$ and $\mathbf{l}_{F,h} = [l_{F,h+1}, \dots, l_{F,h+24}]^\top$, and the use of the day-ahead capacity generations $\mathbf{g}_{B,h} = [g_{B,h+1}, \dots, g_{B,h+24}]^\top$ and $\mathbf{g}_{F,h} = [g_{F,h+1}, \dots, g_{F,h+24}]^\top$, should be modeled as binary features θ_{l_B} , θ_{l_F} , θ_{g_B} and θ_{g_F} . In particular, if θ_{f_C} is set to 1, where $f \in \{l, g\}$ and $C \in \{B, F\}$, the corresponding time series vector $\mathbf{x}_{f_C,h} = [f_{C,h+1}, \dots, f_{C,h+24}]^\top$ is used as a model input.

Similarly, for the case of the holidays, the features can also be modeled as binary variables θ_{H_B} and θ_{H_F} . In particular, as the set of 24 hours of a day is either a holiday or not, the holidays are defined as model inputs X_{H_B} , $X_{H_F} \in \{0, 1\}$, with 0 and 1 representing respectively no holiday and holiday. Then, if either θ_{H_B} or θ_{H_F} is set to 1, the corresponding variable, i.e. X_{H_B} or X_{H_F} , is used as model input.

To model the Belgium prices, we need to use an integer feature to select the number of the considered past values. In particular, as the prices display daily and weekly seasonality, we have to use two integer features: $\theta_{p_{B,d}} \in \{1, 2, \dots, 6\}$ as the feature modeling the number of past days during the last week, i.e. modeling daily seasonality, and $\theta_{p_{B,w}} \in \{1, 2, 3\}$ as the feature modeling the number of days at weekly lags, i.e. modeling weekly seasonality. Based on the selection of $\theta_{p_{B,d}}$ and $\theta_{p_{B,w}}$, the

considered EPEX-Belgium past prices can be decomposed as the price inputs $\mathbf{X}_{p_{B,h}}^d$ at daily lags and the price inputs $\mathbf{X}_{p_{B,h}}^w$ at weekly lags:

$$\mathbf{X}_{p_{B,h}}^d = [p_{B,h-i_1}, \dots, p_{B,h-i_{N_d}}]^\top, \quad (19a)$$

$$\mathbf{X}_{p_{B,h}}^w = [p_{B,h-j_1}, \dots, p_{B,h-j_{N_w}}]^\top, \quad (19b)$$

where:

$$\{i_1, \dots, i_{N_d}\} = \{i \mid 0 \leq i \leq 24 \cdot \theta_{p_{B,d}} - 1\} \quad (19c)$$

$$\{j_1, \dots, j_{N_w}\} = \{j \mid 1 \leq k \leq \theta_{p_{B,w}}, \\ k \cdot 168 \cdot \theta_{p_{B,d}} \leq j \leq k \cdot 192 \cdot \theta_{p_{B,d}} - 1\} \quad (19d)$$

It is important to note that, as this is the time series to be predicted, we disregard the cases where no daily nor weekly seasonality is used, i.e. $\theta_{p_{B,d}} = 0$ or $\theta_{p_{B,w}} = 0$.

Finally, for the EPEX-France prices we could use the same integer features as for EPEX-Belgium. However, for simplicity, we directly consider the same lags for both time series and model the French prices as a binary feature θ_{p_F} . It is important to note that, despite having the same length, the selection of both time series is still independent; particularly, the lags are only defined for Belgium, and the French prices are just excluded or included. The modeled input features are summarized in Table 1.

Feature	Domain	Definition
$\theta_{p_{B,d}}$	$\{1, \dots, 6\}$	Number of past days for input price sequence
$\theta_{p_{B,w}}$	$\{1, \dots, 3\}$	Days at weekly lags for input price sequence
θ_{p_F}	$\{0, 1\}$	Day-ahead price in France
θ_{l_B}	$\{0, 1\}$	Load in Belgium
θ_{l_F}	$\{0, 1\}$	Load in France
θ_{g_B}	$\{0, 1\}$	Generation in Belgium
θ_{g_F}	$\{0, 1\}$	Generation in France
θ_{H_B}	$\{0, 1\}$	Holidays in Belgium
θ_{H_F}	$\{0, 1\}$	Holidays in France

Table 1: Definition of the modeled input features.

5.2.2. Hyperparameter Optimization

In order to guarantee that the network is adapted according to the input size, we simultaneously optimize the hyperparameters of the DNN, i.e. the number of neurons n_1 and n_2 . In particular, as the

feature selection method is based on a hyperparameter optimization, we directly include the number of neurons as integer hyperparameters that are optimized together with the features. We set the domain of n_1 as the set of integers $\{100, 101, \dots, 400\}$ and the one of n_2 as $\{0\} \cup \{48, 49, \dots, 360\}$, where $n_2 = 0$ represents removing the second hidden layer and using a network of depth one. It is important to note that, while allowing the removal of a hidden layer modifies the model proposed in Section 3, it is done to guarantee that the addition of a second hidden layer, as proposed by [23], is indeed necessary to enhance the performance.

5.2.3. Experimental Setup

In order to use the proposed algorithm, we first need to define the threshold ϵ for the minimum variance contribution; in our case, we select $\epsilon = 0.5\%$. In addition, we also need to select the maximum number of iterations T of the TPE algorithm; we found $T = 1000$ to offer a good trade-off between performance and accuracy. Particularly, considering that training a single model takes 2 min, the full feature selection requires 30 h. While this might seem a long time, this step is only performed after some periodic time, e.g. a month, to reassess feature dependencies; therefore, the proposed approach and settings yield a feasible and accurate method for the time scale of day-ahead prices.

For implementing the functional analysis of variance, we use the python library fANOVA developed by the authors of [40]. Likewise, for implementing the TPE algorithm, we use the python library hyperopt [66].

5.2.4. Feature Selection Results

In a first conducted experiment, we obtained an unexpected result: inclusion/exclusion of the generation capacity in Belgium g_B accounts for roughly 75% of the performance variance \mathbb{V} , with inclusion of g_B dramatically decreasing the predictive accuracy. Since the generation capacity has been successfully used by other authors as a market driver [2], this result requires some explanation. From Figure 6, which displays the time series of g_B , we can comprehend the result: right before the transition from the training to the validation set, the average g_B suffers a major change and drops from approximately 14 GW to 9 GW. Because of the drastic drop, it is likely that some relations that are learned based on the training set, do not hold in the validation set, and that as a result, the predictive per-

formance in the validation set worsens when g_B is considered.

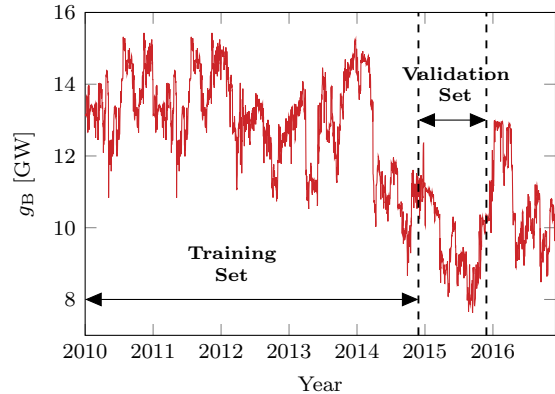


Figure 6: Generation in Belgium in the considered period.

This regime change in g_B violates the assumption that conditions in the training, validation, and test sets are equal. Therefore, to perform a correct feature selection and to guarantee that the three datasets hold similar conditions, the experimental setup should disregard θ_{g_B} . It is important to note that, before taking this decision, we have considered shuffling the data to ensure homogeneous conditions between the three sets. However, this alternative was avoided for two reasons:

- As the output prices in some samples are the input features in others, data has to be discarded in order to avoid data contamination between the three sets. As a result, since the larger the dataset the better the DNN can generalize, this implementation could potentially decrease the predictive accuracy of the model.
- In addition, since the end goal of the model is to forecast recent prices, it would be meaningless to try to model an input-output relation that no longer holds.

Considering these facts, a correct feature selection is performed without θ_{g_B} . As depicted in Table 2, the first result to be noted from the new experimental results is that, as g_B is a big source of error, the variance $\hat{\mathbb{V}}$ of the sMAPE performance is reduced by a factor of 5. In addition, as it could be expected, the results obtained in this new experiment display a more distributed contribution among the different features. In particular, in the first experiment, g_B was responsible for 75% of the

	$\hat{\mathbb{V}}$
Feature selection with g_B	0.58 % ²
Feature selection without g_B	0.12 % ²

Table 2: Performance variance with and without g_B .

performance variance. Now, as depicted in Table 3, French prices and load account for roughly 50 % of the total performance variance, and the available generation in France, the load in Belgium, and the number of past days play a minor role.

	Contribution to \mathbb{V}
All main effects	64.9%
French load	28.4%
French prices	25.7%
French generation	4.78%
Belgium load	1.0%
Past days number	0.8%

Table 3: Variance contribution of single features for the second feature selection experiment.

Based on the above results, we can make a first selection and remove from the set of possible inputs the holidays θ_{H_B} and θ_{H_F} as both seem not to be decisive. Similarly, we can select $\theta_{p_{B,w}} = 1$ as the number of days at weekly lags seems to be non-critical. Finally, to complete the feature selection, we should use the marginal performances of the five important features represented in Figure 7; based on them, it is clear that we should select the price, load and generation in France, discard the grid load in Belgium, and use two days of past price data.

5.2.5. Hyperparameter Selection Results

The obtained hyperparameter results are depicted in Table 4 and Figure 8. When comparing them with the results depicted in Table 3 and Figure 7, it seems that the network structure is less important than the selected features. However, despite not being the most important factor, it is clear that a second hidden layer is beneficial; particularly, we can clearly see how from one hidden layer, i.e. $n_2 = 0$, the performance continuously improves until a plateau around $n_2 = 200$ neurons is reached. For n_1 , while its contribution is much less noticeable than the one of n_2 , increasing the number of

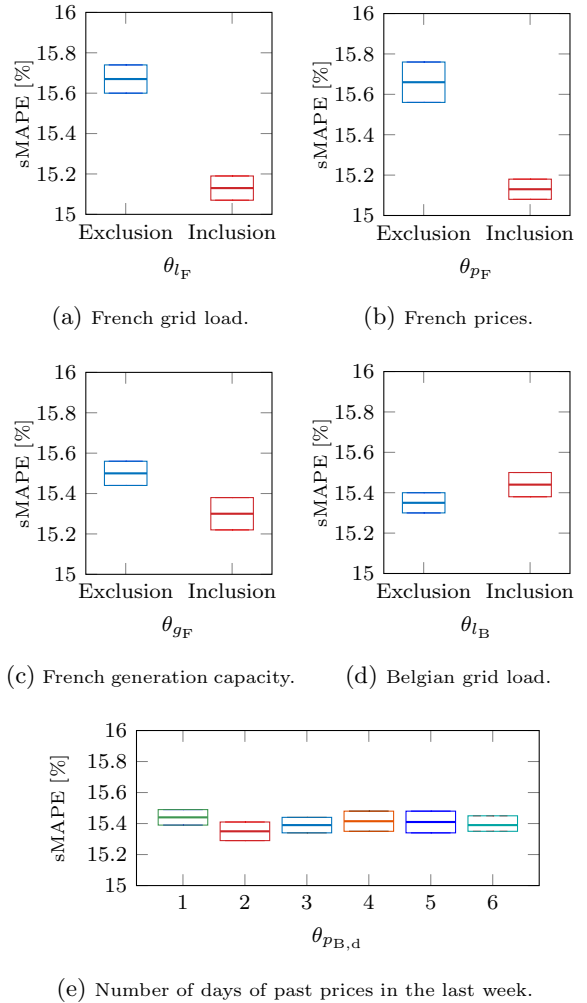


Figure 7: Marginal performance on the validation set of the five most important features.

neurons until $n_1 = 300 - 350$ seems to slightly improve the performance.

5.3. Discussion

Based on the results of the feature selection algorithm, we include the following features as model inputs:

1. Day-ahead load and generation in France:

$$\mathbf{X}_{l_F,h} = [l_{F_{h+1}}, l_{F_{h+2}}, \dots, l_{F_{h+24}}]^\top, \quad (20a)$$

$$\mathbf{X}_{g_F,h} = [g_{F_{h+1}}, g_{F_{h+2}}, \dots, g_{F_{h+24}}]^\top. \quad (20b)$$

2. Last two days of Belgian and French prices:

$$\mathbf{X}_{p_{B,h}}^d = [p_{B_{h-0}}, p_{B_{h-1}}, \dots, p_{B_{h-47}}]^\top, \quad (20c)$$

$$\mathbf{X}_{p_{F,h}}^d = [p_{F_{h-0}}, p_{F_{h-1}}, \dots, p_{F_{h-47}}]^\top. \quad (20d)$$

	Contribution to \mathbb{V}
n_1	0.8%
n_2	1.1%

Table 4: Variance contribution of the network structure.

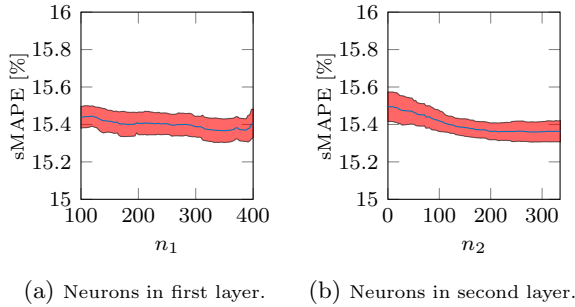


Figure 8: Marginal performance of the hyperparameters.

3. Belgian and French prices a week before:

$$\mathbf{X}_{p_{B,h}}^w = [p_{B_{h-168}}, p_{B_{h-169}}, \dots, p_{B_{h-191}}]^\top, \quad (20e)$$

$$\mathbf{X}_{p_{F,h}}^w = [p_{F_{h-168}}, p_{F_{h-169}}, \dots, p_{F_{h-191}}]^\top. \quad (20f)$$

In addition, while it seems that the different French market features play a large role in the forecasting accuracy, the results are only enough to have a general idea of the importance of French data; particularly, a statistical analysis is required before making any further conclusion.

Finally, while we have used the proposed algorithm to select the input features, we have not yet provided an evaluation of its accuracy. In particular, to assess its performance, we could compare models using only optimally selected features against models using also features that have been discarded; specifically, we could evaluate the difference in predictive accuracy by means of hypothesis testing. However, since hypothesis testing and results for different models are already presented in the next section, we leave this evaluation for Section 6.2.4.

6. Case Study - Part II: Modeling Framework Evaluation

As stated through the different parts of the paper, the main goal of this research is to propose different models for including market integration in day-ahead forecasting, and then, to illustrate how

market integration improves the predictive accuracy of price forecasting. While the models are already proposed in Section 3, and while we are able to use the results of the feature selection to obtain a first qualitative assessment of the effect of market integration, a deeper study is still required.

In particular, the analysis provided by the feature selection algorithm is based on the validation set; while this dataset is not used for training the network, it is employed for early stopping and hyperparameter optimization. Therefore, to have a fully fair and unbiased evaluation, we need an extra comparison using unseen data to the full training process. In addition, the previous results were obtained using the first proposed model; therefore, results for the other two models are still required. Finally, to have a meaningful and complete assessment, statistical significance of the results has to be obtained. To accomplish the analysis and fulfill the requirements, the goal of this section is threefold:

1. Provide statistical significance of the improvements of using French market data by performing a DM test on the out-of-sample data represented by the test set.
2. Based on the same statistical test, demonstrate how a dual-market forecasters can provide significant improvements in predictive accuracy.
3. Show how a model that predicts spikes can be used to enhance the forecasting performance.

Based on them, the section is organized as follows: Section 6.1 describes the DM test applied to our case study. Next, Section 6.2 performs the statistical analysis on the importance of market integration using the first proposed model. Then, Section 6.3 and 6.4 repeat the statistical analysis but applied respectively to the second and third proposed models. Finally, Section 6.5 provides a discussion on the obtained results.

6.1. Diebold-Mariano Test

To assess the statistical significance in the difference of predictive accuracy, we use the DM test as defined by (6)-(9). In particular, since the neural network is trained using the absolute mean error, we choose to use also the absolute error to build the loss differential:

$$d_k^{M_1, M_2} = |\varepsilon_k^{M_1}| - |\varepsilon_k^{M_2}|. \quad (21)$$

In addition, we follow the same procedure as in [29, 67] and we perform an independent DM test

for each of the 24 time series representing the different hours of a day. The reason for this is that, as we use the same information to forecast the set of 24 prices, the forecast errors within the same day would exhibit a high correlation. Moreover, to have an assessment of the whole error sequence, we also perform the DM test considering serial correlation of order k in the error sequence. Particularly, recalling that optimal k -step-ahead forecast errors are at most $(k - 1)$ -dependent [50], we perform a DM test on the full loss differential considering serial correlation of order 23.

In the various experimental setups of this case study, we employ the one-sided DM test given by (8) at the 95% confidence level. This selection is done because we want to study whether the performance of a forecaster A is statistically significantly better than a forecaster B, not whether the performances of forecasters A and B are significantly different (like it would be the case in the two-sided DM test). In more detail, for each hour $h = 1, \dots, 24$ of the day, we test the null hypothesis of a model M_1 that uses French data having the same or worse accuracy than a model M_2 that uses no French data. More specifically, we perform the following tests:

$$\begin{cases} H_0 : \mathbb{E}(d_{h_k}^{M_1, M_2}) \geq 0, \\ H_1 : \mathbb{E}(d_{h_k}^{M_1, M_2}) < 0, \end{cases} \quad \text{for } h = 1, \dots, 24, \quad (22)$$

where $[d_{h_1}, \dots, d_{h_{N/24}}]^\top$ represents the vector sequence of loss differentials of hour h . In addition, we perform the same test but considering the full loss differential sequence and assuming serial correlation:

$$\begin{cases} H_0 : \mathbb{E}(d_k^{M_1, M_2}) \geq 0, \\ H_1 : \mathbb{E}(d_k^{M_1, M_2}) < 0. \end{cases} \quad (23)$$

6.2. French Market Data: Statistical Significance

In Section 5.2-5.3, we have showed that using market data from connected markets can help to improve the performance. In this section, we extend the analysis by directly comparing a model that includes this type of data against a model that excludes it, and then, performing a DM test to analyze the statistical significance.

6.2.1. Experimental Setup

The model used to perform the evaluation is the single-market forecaster employed for the fea-

ture selection. In particular, based on the obtained hyperparameter results, we select $n_1 = 320$ and $n_2 = 200$; similarly, considering the optimized prices lags obtained in the feature selection, we consider, as input sequence for the model, the Belgium prices during the last two days and a week before. Furthermore, we discard as input features the capacity generation in Belgium as well as the holidays in both countries. Then, in order compare the effect of French data, we consider the remaining features as possible inputs for the model; i.e., we compare the first model excluding all the French data and only considering Belgian prices with respect to the second model including the French data. We respectively refer to these two models by M_{NoFR} and M_{FR} .

In addition, while the load in Belgium l_B appears to be non-relevant, we decided to repeat the previous experiment but including l_B in both models. The reason for this is twofold:

1. By adding the Belgian load, we ensure that the good results of using French data are not due to the fact that the model does not include specific Belgian regressors.
2. Furthermore, with this experiment, we can also validate the results of the feature selection algorithm. In particular, as the load does not seem to play a big role, we expect the performance difference between models with and without l_B to be insignificant.

Similar as before, we refer to these models by M_{NoFR, l_B} and M_{FR, l_B} . For the sake of visualization, Table 5 and 6 respectively display the common and different hyperparameters/features of the four models.

n_1	n_2	$\theta_{p_{B,d}}$	$\theta_{p_{B,w}}$	θ_{g_B}	θ_{H_B}	θ_{H_F}
320	200	2	1	0	0	0

Table 5: Common hyperparameters and features of the four considered models.

6.2.2. Case 1: Models Without l_B

In this experiment, we compare M_{NoFR} against M_{FR} by evaluating their performance on the year of yet unused data represented by the test set. As in a real world application, to account for the last available information, the two models are re-estimated after a number days/weeks. In our application, considering that a model takes around 2 minutes to be

Feature	M_{NoFR}	M_{FR}	$M_{\text{NoFR},l_{\text{B}}}$	$M_{\text{FR},l_{\text{B}}}$
$\theta_{p_{\text{F}}}$	0	1	0	1
$\theta_{l_{\text{B}}}$	0	0	1	1
$\theta_{l_{\text{F}}}$	0	1	0	1
$\theta_{g_{\text{F}}}$	0	1	0	1

Table 6: Differences among the models in input features.

trained on the GPU, we decide to re-estimate them using the smallest possible period of a day.

A first comparison of the models is obtained from Table 7 where the sMAPE for the test set is listed for both models. From this first evaluation, we can see that including the French data seems to really enhance the performance of the forecaster.

Model	M_{NoFR}	M_{FR}
sMAPE	16.0%	13.2%

Table 7: Performance comparison between M_{NoFR} and M_{FR} in the out-of-sample data in terms of sMAPE.

To provide statistical significance to the above result, we perform a DM test as described in Section 6.1. The obtained results are depicted in Figure 9, where the test statistic is represented for each of the 24 hours of a day and where the points above the dashed line accept, at a 95 % confidence, the alternative hypothesis of M_{FR} having better performance accuracy.

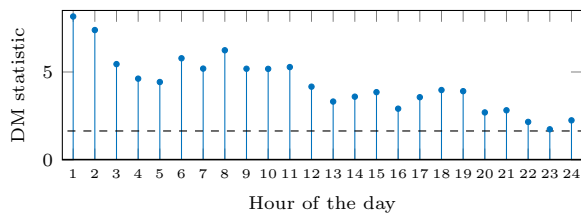


Figure 9: DM test results when comparing M_{NoFR} and M_{FR} . Values above the dashed line reject the null hypothesis with a 95 % confidence level, and in turn, represent cases where the accuracy of M_{FR} is significantly better.

As we can see from the plot, the forecast improvements of the model M_{FR} including French data are statistically significant for each one of the 24 day-ahead prices. In particular, when we look at Table 8 displaying the respective p -values, i.e. the probability of observing the obtained error sequences given

that H_0 is true, we can see that all the p -values are below the 0.05 threshold to be statistically significant at 95 % confidence level.

Hour	h₁	h₂	h₃	h₄
p-value	$1.7 \cdot 10^{-16}$	$7.6 \cdot 10^{-14}$	$2.5 \cdot 10^{-08}$	$1.9 \cdot 10^{-06}$
Hour	h₅	h₆	h₇	h₈
p-value	$4.7 \cdot 10^{-06}$	$3.7 \cdot 10^{-09}$	$1.0 \cdot 10^{-07}$	$2.3 \cdot 10^{-10}$
Hour	h₉	h₁₀	h₁₁	h₁₂
p-value	$1.1 \cdot 10^{-07}$	$1.1 \cdot 10^{-07}$	$6.5 \cdot 10^{-08}$	$1.6 \cdot 10^{-05}$
Hour	h₁₃	h₁₄	h₁₅	h₁₆
p-value	$4.5 \cdot 10^{-04}$	$1.6 \cdot 10^{-04}$	$5.8 \cdot 10^{-05}$	$1.8 \cdot 10^{-03}$
Hour	h₁₇	h₁₈	h₁₉	h₂₀
p-value	$1.8 \cdot 10^{-04}$	$3.5 \cdot 10^{-05}$	$4.6 \cdot 10^{-05}$	$3.5 \cdot 10^{-03}$
Hour	h₂₁	h₂₂	h₂₃	h₂₄
p-value	$2.4 \cdot 10^{-03}$	0.015	0.041	0.012

Table 8: p -values at each day-ahead hour for the DM test comparing M_{NoFR} and M_{FR} . Values below 0.05 represent cases where the accuracy of M_{FR} is significantly better.

When the DM test is performed on the full loss differential and taking into account serial correlation, the obtained metrics completely agree with the results obtained for the individual 24 hours. In particular, as displayed in Table 9, a p -value of $1.2 \cdot 10^{-11}$ confirms the strong statistical significance of using the French data in the prediction model.

p -value	DM Statistic
$1.2 \cdot 10^{-11}$	6.67

Table 9: p -value and statistic for the DM test on the full loss differential between M_{NoFR} and M_{FR} .

6.2.3. Case 2: Models with l_{B}

We repeat the same evaluation but comparing $M_{\text{NoFR},l_{\text{B}}}$ against $M_{\text{FR},l_{\text{B}}}$. From Table 10 we can see how, as before, in terms of sMAPE, the model including French data outperforms the alternative.

Model	$M_{\text{NoFR},l_{\text{B}}}$	$M_{\text{FR},l_{\text{B}}}$
sMAPE	15.7%	13.1%

Table 10: Performance comparison between $M_{\text{NoFR},l_{\text{B}}}$ and $M_{\text{FR},l_{\text{B}}}$ in the out-of-sample data in terms of sMAPE.

To provide statistical significance to the obtained accuracy difference we again perform the DM tests. The obtained results are illustrated in Figure 10;

as before, including French data leads to improvements in accuracy that are statistically significant for the 24 predicted values.

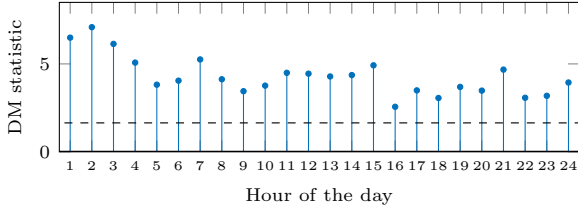


Figure 10: DM test results when comparing M_{NoFR,l_B} and M_{FR,l_B} . Values above the dashed line reject the null hypothesis at a 5% significance level, and in turn, represent cases where the accuracy of M_{FR,l_B} is significantly better.

For the sake of simplicity, as the results depicted in Figure 10 are rather conclusive, we avoid the representation of the large table of individual p -values. However, we note that the p -value of considering the full loss differential with serial correlation is $1.6 \cdot 10^{-12}$, a value that agrees with Figure 10 and confirms once more that the improvements of using French data are statistically significant.

6.2.4. Accuracy of the Feature Selection

Using the results of the previous two sections, we can illustrate the accuracy of the proposed feature selection algorithm in Section 4. In particular, when performing the feature selection, we have observed that the contribution of the Belgian load l_B was rather insignificant and even slightly negative; this led, in turn, to discard l_B as an input feature. In this section, to verify that the selection algorithm performed the right choice by avoiding l_B , we perform two DM tests to compare M_{NoFR,l_B} against M_{NoFR} and M_{FR,l_B} against M_{FR} . In particular, we perform a two-sided DM test per model pair with the null hypothesis of the models having equal accuracy.

For the sake of simplicity, we avoid depicting the DM test results for each individual hour; instead we directly illustrate the p -values of the DM test when considering the whole loss differential sequence with serial correlation. As can be seen from Table 11, the obtained p -values for both tests are above 0.05, and as a result, the null hypothesis of equal accuracy cannot be rejected, i.e. there is no statistical evidence of the models using Belgian load having different accuracy than the models without it.

Based on the obtained results, it is clear that using l_B is not important, and thus, that the choice

Model Pair	p -value
M_{FR,l_B} vs M_{FR}	0.435
M_{NoFR,l_B} vs M_{NoFR}	0.275

Table 11: p -values for DM test with the null hypothesis of models with l_B having equal accuracy as models without it.

performed by the feature selection algorithm is correct. In particular, while this experiment does not analyze the performance of the feature selection on all the inputs, it does consider the most problematic feature. Specifically, as many researchers have successfully used the load as an explanatory variable [5, 9, 10, 30, 36, 68] and as the load itself does not display any regime change in the considered time interval, it is rather striking to see its minimal effect on the performance. Therefore, by demonstrating that the algorithm is correct when discarding the load, we obtain an assessment of its general accuracy, and we can conclude that the algorithm performs a correct feature selection.

6.3. Evaluation of a Dual-Market Forecaster

In this section, to test the accuracy and the possible improvements of using this dual-market forecaster, we perform a comparison between the single model predicting the 24 day-ahead prices in Belgium and the dual-market forecaster predicting the set of 48 prices in Belgium and France. In particular, the models are denoted by M_{Single} and M_{Dual} , and they both use the optimal features and hyperparameters obtained for the single model in Section 4. It is important to note that, while in an ideal experiment the hyperparameters of the dual-market forecaster should be re-estimated, for simplicity we decide to directly use the hyperparameters obtained for the single-market forecaster.

As before, the models are evaluated using the test set and to account for the last available information they are re-estimated on a daily basis. Similar as in the previous section, we first provide in Table 12 a model comparison in terms of sMAPE. From this first evaluation, it seems that using dual-market forecasts can improve the performance.

To provide statistical significance to these results, we again perform the DM test for each of the 24 hours of a day. The obtained statistics are depicted in Figure 11; as before, the points above the upper dashed line accept, at a 95 % confidence, the

Model	M_{Single}	M_{Dual}
sMAPE	13.2%	12.5%

Table 12: Performance comparison between the single and dual-market forecasters in terms of sMAPE.

alternative hypothesis of M_{Dual} having a better performance accuracy. In addition, as not every hourly forecast is statistically significant, we represent in the same figure the alternative DM test with the null hypothesis of M_{Single} having equal or lower accuracy than M_{Dual} . This test is characterized by the lower dashed line and any point below this line accepts at a 95 % confidence that M_{Single} has better performance accuracy.

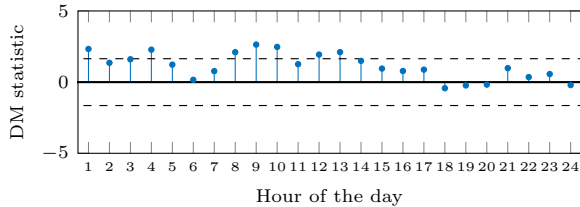


Figure 11: DM test results when comparing M_{Single} and M_{Dual} . Values above the top dashed line represent cases where, with a 95 % confidence level, M_{Dual} is significantly better. Similarly, values below the lower dashed line accept at a 95 % confidence level that M_{Dual} is significantly worse.

As we can see from the plot, the forecast improvements of the dual-market forecaster are statistically significant in 7 of the 24 day-ahead prices. In addition, the single-market forecaster is not significantly better in any of the remaining 17 day-ahead prices. Therefore, as M_{Dual} is approximately better for a third of the day-ahead prices and not worse for the remaining two-thirds, we can conclude that the dual-market forecaster is a statistically significant better forecaster.

For the sake of completeness, we also include Table 13 displaying the respective p -values. It is important to note that, while p -values below 0.05 represent points where M_{Dual} is significantly better, p -values above 0.95 represent points where M_{Single} is significantly better. As already observed from Figure 11, M_{Dual} is significantly better in 7 of 24 day-ahead prices and not significantly worse in the rest.

Finally, as before, we also perform the DM test on the full loss differential taking into account se-

Hour	h_1	h_2	h_3	h_4
p-value	$9.9 \cdot 10^{-03}$	$8.7 \cdot 10^{-02}$	$5.4 \cdot 10^{-02}$	$1.1 \cdot 10^{-02}$
Hour	h_5	h_6	h_7	h_8
p-value	$1.0 \cdot 10^{-01}$	$4.3 \cdot 10^{-01}$	$2.2 \cdot 10^{-01}$	$1.8 \cdot 10^{-02}$
Hour	h_9	h_{10}	h_{11}	h_{12}
p-value	$4.2 \cdot 10^{-03}$	$6.7 \cdot 10^{-03}$	$1.0 \cdot 10^{-01}$	$2.6 \cdot 10^{-02}$
Hour	h_{13}	h_{14}	h_{15}	h_{16}
p-value	$1.8 \cdot 10^{-02}$	$6.7 \cdot 10^{-02}$	$1.7 \cdot 10^{-01}$	$2.2 \cdot 10^{-01}$
Hour	h_{17}	h_{18}	h_{19}	h_{20}
p-value	$1.9 \cdot 10^{-01}$	$6.7 \cdot 10^{-01}$	$5.9 \cdot 10^{-01}$	$5.7 \cdot 10^{-01}$
Hour	h_{21}	h_{22}	h_{23}	h_{24}
p-value	$1.6 \cdot 10^{-01}$	$3.6 \cdot 10^{-01}$	$2.9 \cdot 10^{-01}$	$5.8 \cdot 10^{-01}$

Table 13: p -values when comparing M_{Dual} and M_{Single} . Values below $5 \cdot 10^{-02}$ represent cases where the accuracy of M_{Dual} is significantly better. Values above $9.5 \cdot 10^{-01}$ represent cases where M_{Single} is significantly better.

rial correlation. Once again, the obtained metrics agree with the results obtained for the individual 24 hours; particularly, as displayed in Table 14, the obtained p -value is $9.5 \cdot 10^{-03}$ and confirms the statistical significance of the difference in predictive accuracy when using the dual-market forecaster.

p-value	DM Statistic
$9.5 \cdot 10^{-03}$	2.3

Table 14: p -value and statistic for the DM test comparing the full loss differential with serial correlation between M_{Dual} and M_{Single} .

6.4. Model for Spike Detection

In Section 3, we have proposed a model to predict the probability of price spikes and we have indicated that it could be used as an input in the main price forecasters in order to improve the predictive accuracy. As a result, the goal of this section is to, first, outline the obtained results in spike detection, and then, illustrate the performance improvements when using the output of this new model as an input feature of the price forecasters.

6.4.1. Spike Detection

Two models are trained to detect the spikes in the EPEX-Belgium and the EPEX-France. These models are respectively referred to as M_{BSpike} and M_{FSpike} . The configuration used is the same in both scenarios: a DNN with $n_1 = 48$ and $n_2 = 24$ neurons. As input features, both models use the grid

load l , the generation capacity g , and the ratio l/g of the market they are forecasting, i.e. French (Belgian) data is not used to train the model predicting Belgian (French) spikes. In addition, the hyperparameter μ balancing the number of outliers is chosen as 200.

It is important to note that, as we observed that the final classification performance highly depends on the initial weights, the hyperparameters and input features are not guaranteed to be selected optimally. In particular, as the optimization problem to train the network is highly non-convex, multi-start optimization is required to obtain a good classification accuracy. As a result, to optimally select the hyperparameters and features, we would ideally perform a hyperparameter optimization for each one of the multi-start points. Nevertheless, as this method is not computationally tractable, we decided instead to test 20 reasonable network configurations on the validation set; more specifically, for each one of the 20 networks, we solve a multi-start optimization problem with 100 different starting points that are randomly initialized using the Glorot uniform initialization [51]. Then, among all the local minima, the best one is selected as the optimal network configuration.

The results of the two models on the validation set are depicted in Table 15. Negative misclassification refers to wrongly predicting an outlier when there is none; likewise, positive misclassification describes the situation when there is an outlier but the model does not predict it. It is important to point out that the results displayed below consider an outlier as a binary variable by assuming that an outlier takes place if it is predicted probability is higher than 0.5.

Model	Positive misclassification	Negative misclassification
M_{BSpike}	20.00 %	9.43 %
M_{FSpike}	8.57 %	6.54 %

Table 15: Misclassification error of the spike probability forecasters.

As observed from the table, the French model is able to predict outliers with classification errors below 10 %. Similarly, in the case of Belgium prices, the model detects outliers with classification errors below 20 %.

6.4.2. Improving Price Forecasting Accuracy

As explained before, once the models are trained, we can use them as input features for the main forecaster. However, as the underlying idea of each model is different, their effect must be studied separately. In particular, prediction of outliers in Belgium is directly used to enhance predictive accuracy of Belgian prices when the dynamics are spiky. By contrast, prediction of outliers in France is studied as a market integration feature that can improve the forecasting in Belgian prices.

Belgian Spike Prediction

To test the importance of using the output of M_{BSpike} as an input feature, we consider the optimal model M_{NoFR} as defined in Section 6.2.2. Then, we compare its performance against $M_{\text{NoFR}_{\text{Spike}}}$, a model modification that has the exact same configuration but uses as input the predictions of M_{BSpike} . As always, a first sMAPE comparison is depicted in Table 16. From it, we can observe that the model considering spike probability seems to perform better.

Model	M_{NoFR}	$M_{\text{NoFR}_{\text{Spike}}}$
sMAPE	16.0%	15.3%

Table 16: Comparison between model with and without Belgian spike probability in terms of sMAPE.

To test the significance of the improvement, the DM test results for each hour are represented in Figure 12. As can be observed, the forecasting improvements are statistically significant for 13 of the 24 hours and not significantly worse for the rest. This result agrees with the DM test performed in the full loss differential, which, with a p -value of 0.001, indicates that the improvements of using spike predictions in the Belgian market are statistically significant.

From these results, it is important to remark that, while the load and generation in Belgium do not improve the predictive accuracy when used in the main forecasters, they do help to predict outliers in the Belgian market and these predictions improve the predictive accuracy. A possible explanation for this effect is that, while the dynamics of Belgian prices are mostly determined by French features, anomalies in the load/generation in Belgium do influence the price dynamics in the form of spikes.

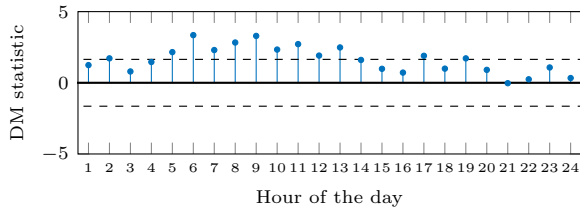


Figure 12: DM test results when comparing M_{NoFR} and $M_{\text{NoFR}_{\text{Spike}}}$. Values above the top dashed line represent cases where the accuracy of $M_{\text{NoFR}_{\text{Spike}}}$ is significantly better

French Spike Prediction

Similar to the previous section, we regard the optimal model M_{FR} and compare it against $M_{\text{FR}_{\text{Spike}}}$, a modification with the same configuration but using as input the predictions of M_{FSpike} . The sMAPE comparison is given in Table 17, and from the results we can observe how using French outliers leads to a minor improvement.

Model	M_{FR}	$M_{\text{FR}_{\text{Spike}}}$
sMAPE	13.2%	12.9%

Table 17: Comparison between model with and without French spike probability in terms of sMAPE.

Nevertheless, in spite of the sMAPE results, the obtained improvements are not statistically significant. In particular, the DM test performed in the full loss differential exhibits a p -value of 0.56, a result that indicates that the improvements are not statistically significant. In addition, the 24 individual hourly p -values are also above the 0.05 threshold. Therefore, while it seems that French outliers improve accuracy, there is no strong evidence to support the claim. As a consequence, we cannot know whether using French outliers helps to improve the predictive accuracy.

6.5. Analysis and Discussion

From the obtained results in the previous sections, we can conclude the following:

1. Using features from the French market significantly enhances the predictive accuracy of a model forecasting Belgian prices. The results are statistically significant and independent of whether Belgian features are considered or not.

2. A dual-market forecaster simultaneously predicting prices in France and Belgium can improve the predictive accuracy. In particular, by solving two related tasks, it is able to learn more useful features, generalize better the price dynamics, and obtain improvements that are statistically significant.
3. By predicting outliers, the forecasting accuracy can also be enhanced. In particular, by using the probabilities of outliers occurring in France and Belgium, the predictive accuracy of Belgian prices displays improvements. In the case of Belgian outliers, the improvements are statistically significant.
4. The proposed feature selection algorithm is able to perform a correct assessment of the importance of features.

In addition, while not being the main results of the analysis, it is interesting to see how explanatory variables from the EPEX-Belgium, e.g. load and generation, have almost no influence in the day-ahead prices. In fact, from the obtained results, it is surprising to observe how French factors play a larger role in Belgian prices than the local Belgian features.

As a final remark, it is necessary to indicate why, while being neighboring countries of Belgium, The Netherlands and Germany and their respective markets are not considered in the study. A common reason to both markets is the fact that, by considering a single neighboring country, effects due to market integration are easier to analyze. A second reason for not considering The Netherlands is the fact that the amount of available online data is smaller than in France and Belgium, and thus, training the DNNs can be harder. In the case of Germany, another reason for not considering it is that, at the moment, there is not a direct interconnection of the electrical grid between Belgium and Germany.

7. Conclusions

We have analyzed how market integration can be used to enhance the predictive accuracy of day-ahead price forecasting in electricity markets. In particular, we have proposed a first model that, by considering features from connected markets, improves the predictive performance. In addition, we have proposed a dual-market forecaster that, by

multitasking and due to market integration, can further improve the predictive accuracy.

As a case study, we have considered the electricity markets in Belgium and France. Then, we have showed how, considering market integration, the proposed forecasters lead to improvements that are statistically significant.

Additionally, we have proposed a novel feature selection algorithm; then, using the same case study, we have showed how the algorithm correctly assesses feature importance. Finally, we have also demonstrated how spike detection can improve predictive accuracy.

In future work, the performed experiments will be expanded to other markets. In particular, as the data used for this experiment is available online for other European markets, evaluating the suitability of the proposed methods should be relatively easy and an interesting topic for future research.

Acknowledgment

This research has received funding from the European Union's Horizon 2020 research and innovation program under the Marie Skłodowska-Curie grant agreement No 675318 (INCITE).

References

References

- [1] M. Shahidehpour, H. Yamin, Z. Li, Market overview in electric power systems, in: *Market Operations in Electric Power Systems*, John Wiley & Sons, Inc., New York, USA, 2002, Ch. 1, pp. 1–20. doi:10.1002/047122412X.ch1.
- [2] R. Weron, Electricity price forecasting: A review of the state-of-the-art with a look into the future, *International Journal of Forecasting* 30 (4) (2014) 1030–1081. doi:10.1016/j.ijforecast.2014.08.008.
- [3] S. K. Aggarwal, L. M. Saini, A. Kumar, Electricity price forecasting in deregulated markets: A review and evaluation, *International Journal of Electrical Power & Energy Systems* 31 (1) (2009) 13–22. doi:10.1016/j.ijepes.2008.09.003.
- [4] T. Jamasb, M. Pollitt, Electricity market reform in the European union: review of progress toward liberalization & integration, *The Energy Journal* 26 (Special Issue) (2005) 11–41. doi:10.5547/issn0195-6574-ej-vol26-nosi-2.
- [5] F. J. Nogales, J. Contreras, A. J. Conejo, R. Espínola, Forecasting next-day electricity prices by time series models, *IEEE Transactions on Power Systems* 17 (2) (2002) 342–348. doi:10.1109/MPER.2002.4312063.
- [6] R. Weron, A. Misiorek, Forecasting spot electricity prices: A comparison of parametric and semiparametric time series models, *International Journal of Forecasting* 24 (4) (2008) 744–763. doi:10.1016/j.ijforecast.2008.08.004.
- [7] A. Conejo, M. Plazas, R. Espínola, A. Molina, Day-ahead electricity price forecasting using the wavelet transform and ARIMA models, *IEEE Transactions on Power Systems* 20 (2) (2005) 1035–1042. doi:10.1109/TPWRS.2005.846054.
- [8] A. J. Conejo, J. Contreras, R. Espínola, M. A. Plazas, Forecasting electricity prices for a day-ahead pool-based electric energy market, *International Journal of Forecasting* 21 (3) (2005) 435–462. doi:10.1016/j.ijforecast.2004.12.005.
- [9] A. Cruz, A. Muñoz, J. Zamora, R. Espínola, The effect of wind generation and weekday on Spanish electricity spot price forecasting, *Electric Power Systems Research* 81 (10) (2011) 1924–1935. doi:10.1016/j.epsr.2011.06.002.
- [10] A. Misiorek, S. Trueck, R. Weron, Point and interval forecasting of spot electricity prices: Linear vs. non-linear time series models, *Studies in Nonlinear Dynamics & Econometrics* 10 (3) (2006) 1–36. doi:10.2202/1558-3708.1362.
- [11] J. M. Vilar, R. Cao, G. Aneiros, Forecasting next-day electricity demand and price using nonparametric functional methods, *International Journal of Electrical Power & Energy Systems* 39 (1) (2012) 48–55. doi:10.1016/j.ijepes.2012.01.004.
- [12] C. R. Knittel, M. R. Roberts, C. Knittel, M. Roberts, An empirical examination of restructured electricity prices, *Energy Economics* 27 (5) (2005) 791–817. doi:10.1016/j.eneco.2004.11.005.
- [13] R. C. Garcia, J. Contreras, M. Van Akkeren, J. B. C. Garcia, A GARCH forecasting model to predict day-ahead electricity prices, *IEEE Transactions on Power Systems* 20 (2) (2005) 867–874. doi:10.1109/tpwrs.2005.846044.
- [14] Z. Tan, J. Zhang, J. Wang, J. Xu, Day-ahead electricity price forecasting using wavelet transform combined with ARIMA and GARCH models, *Applied Energy* 87 (11) (2010) 3606–3610. doi:10.1016/j.apenergy.2010.05.012.
- [15] N. Amjady, M. Hemmati, Energy price forecasting - problems and proposals for such predictions, *IEEE Power and Energy Magazine* 4 (2) (2006) 20–29. doi:10.1109/MPAE.2006.1597990.
- [16] B. Szkuta, L. Sanabria, T. Dillon, Electricity price short-term forecasting using artificial neural networks, *IEEE Transactions on Power Systems* 14 (3) (1999) 851–857. doi:10.1109/59.780895.
- [17] J. P. S. Catalão, S. J. P. S. Mariano, V. M. F. Mendes, L. A. F. M. Ferreira, Short-term electricity prices forecasting in a competitive market: A neural network approach, *Electric Power Systems Research* 77 (10) (2007) 1297–1304. doi:10.1016/j.epsr.2006.09.022.
- [18] S. Fan, C. Mao, L. Chen, Next-day electricity-price forecasting using a hybrid network, *IET Generation, Transmission & Distribution* 1 (1) (2007) 176–182. doi:10.1049/iet-gtd:20060006.
- [19] J. Che, J. Wang, Short-term electricity prices forecasting based on support vector regression and autoregressive integrated moving average modeling, *Energy Conversion and Management* 51 (10) (2010) 1911–1917.

- doi:10.1016/j.enconman.2010.02.023.
- [20] W.-M. Lin, H.-J. Gow, M.-T. Tsai, An enhanced radial basis function network for short-term electricity price forecasting, *Applied Energy* 87 (10) (2010) 3226–3234. doi:10.1016/j.apenergy.2010.04.006.
- [21] M. Shafie-Khah, M. P. Moghaddam, M. Sheikh-El-Eslami, Price forecasting of day-ahead electricity markets using a hybrid forecast method, *Energy Conversion and Management* 52 (5) (2011) 2165–2169. doi:10.1016/j.enconman.2010.10.047.
- [22] N. Amjady, Day-ahead price forecasting of electricity markets by a new fuzzy neural network, *IEEE Transactions on Power Systems* 21 (2) (2006) 887–896. doi:10.1109/tpwrs.2006.873409.
- [23] J. Lago, F. De Ridder, P. Vrancx, B. De Schutter, Forecasting spot electricity prices: deep learning approaches and empirical comparison of traditional algorithms, Technical Report 17-001, Delft Center for Systems and Control, Delft University of Technology, 2017, <https://www.jesuslago.com/forecastingprices/>.
- [24] L. Meeus, R. Belmans, Electricity market integration in Europe, in: *Proceedings of the 16th Power Systems Computation Conference*, 2008.
- [25] D. W. Bunn, A. Gianfreda, Integration and shock transmissions across European electricity forward markets, *Energy Economics* 32 (2) (2010) 278–291. doi:10.1016/j.eneco.2009.09.005.
- [26] L. M. de Menezes, M. A. Houllier, Reassessing the integration of European electricity markets: A fractional cointegration analysis, *Energy Economics* 53 (2016) 132–150. doi:10.1016/j.eneco.2014.10.021.
- [27] G. Zachmann, Electricity wholesale market prices in Europe: Convergence?, *Energy Economics* 30 (4) (2008) 1659–1671. doi:10.1016/j.eneco.2007.07.002.
- [28] E. Lindström, F. Regland, Modeling extreme dependence between European electricity markets, *Energy Economics* 34 (4) (2012) 899–904. doi:10.1016/j.eneco.2012.04.006.
- [29] F. Ziel, R. Steinert, S. Husmann, Forecasting day ahead electricity spot prices: The impact of the EXAA to other European electricity markets, *Energy Economics* 51 (2015) 430–444. doi:10.1016/j.eneco.2015.08.005.
- [30] I. P. Panapakidis, A. S. Dagoumas, Day-ahead electricity price forecasting via the application of artificial neural network based models, *Applied Energy* 172 (2016) 132–151. doi:10.1016/j.apenergy.2016.03.089.
- [31] I. Guyon, A. Elisseeff, An introduction to variable and feature selection, *Journal of Machine Learning Research* 3 (2003) 1157–1182.
- [32] I. Goodfellow, Y. Bengio, A. Courville, *Deep Learning*, MIT Press, 2016, <http://www.deeplearningbook.org/>.
- [33] M. Stevenson, Filtering and forecasting spot electricity prices in the increasingly deregulated australian electricity market, in: *QFRC Research Paper Series*, no. 63, Quantitative Finance Research Centre, University of Technology, Sydney, 2001, http://www.qfrc.uts.edu.au/research/research_papers/rp63.pdf.
- [34] C. P. Rodriguez, G. J. Anders, Energy price forecasting in the Ontario competitive power system market, *IEEE Transactions on Power Systems* 19 (1) (2004) 366–374. doi:10.1109/TPWRS.2003.821470.
- [35] Y.-y. Hong, C.-p. Wu, Day-ahead electricity price forecasting using a hybrid principal component analysis network, *Energies* 5 (11) (2012) 4711–4725. doi:10.3390/en5114711.
- [36] N. Amjady, F. Keynia, Day-ahead price forecasting of electricity markets by mutual information technique and cascaded neuro-evolutionary algorithm, *IEEE Transactions on Power Systems* 24 (1) (2009) 306–318. doi:10.1109/tpwrs.2008.2006997.
- [37] N. Amjady, A. Daraeepour, F. Keynia, Day-ahead electricity price forecasting by modified relief algorithm and hybrid neural network, *IET Generation, Transmission & Distribution* 4 (3) (2010) 432–444. doi:10.1049/iet-gtd.2009.0297.
- [38] D. Keles, J. Scelle, F. Paraschiv, W. Fichtner, Extended forecast methods for day-ahead electricity spot prices applying artificial neural networks, *Applied Energy* 162 (2016) 218–230. doi:10.1016/j.apenergy.2015.09.087.
- [39] O. Abedinia, N. Amjady, H. Zareipour, A new feature selection technique for load and price forecast of electrical power systems, *IEEE Transactions on Power Systems* 32 (1) (2017) 62–74. doi:10.1109/TPWRS.2016.2556620.
- [40] F. Hutter, H. Hoos, K. Leyton-Brown, An efficient approach for assessing hyperparameter importance, in: *Proceedings of the 31st International Conference on International Conference on Machine Learning*, Vol. 32 of ICML’14, 2014, pp. 754–762, <http://proceedings.mlr.press/v32/hutter14.pdf>.
- [41] L. Bottou, Large-scale machine learning with stochastic gradient descent, in: *Proceedings of COMPSTAT’2010*, Physica-Verlag HD, Heidelberg, 2010, pp. 177–186. doi:10.1007/978-3-7908-2604-3_16.
- [42] S. Ruder, An overview of gradient descent optimization algorithms, arXiv eprint (2016). arXiv:1609.04747. URL <https://arxiv.org/abs/1609.04747>
- [43] Y. LeCun, L. Bottou, G. B. Orr, K.-R. Müller, Efficient BackProp, in: G. B. Orr, K.-R. Müller (Eds.), *Neural Networks: Tricks of the Trade*, no. 1524 in *Lecture Notes in Computer Science*, Springer Berlin Heidelberg, 1998, pp. 9–50. doi:10.1007/3-540-49430-8_2.
- [44] R. Gareta, L. M. Romeo, A. Gil, Forecasting of electricity prices with neural networks, *Energy Conversion and Management* 47 (13–14) (2006) 1770–1778. doi:10.1016/j.enconman.2005.10.010.
- [45] D. R. Jones, M. Schonlau, W. J. Welch, Efficient global optimization of expensive black-box functions, *Journal of Global Optimization* 13 (4) (1998) 455–492. doi:10.1023/A:1008306431147.
- [46] J. Bergstra, R. Bardenet, Y. Bengio, B. Kégl, Algorithms for hyper-parameter optimization, in: *Advances in Neural Information Processing Systems*, 2011, pp. 2546–2554, <http://papers.nips.cc/paper/4443-algorithms-for-hyper-parameter>
- [47] F. Hutter, H. H. Hoos, K. Leyton-Brown, Sequential model-based optimization for general algorithm configuration, in: *International Conference on Learning and Intelligent Optimization*, Springer, 2011, pp. 507–523. doi:10.1007/978-3-642-25566-3_40.
- [48] E. Hastie, R. Tibshirani, J. Friedman, *The Elements of Statistical Learning*, Springer Series in Statistics, Springer New York Inc., New York, NY, USA, 2001. doi:10.1007/978-0-387-21606-5.
- [49] S. Makridakis, Accuracy measures: theoretical and practical concerns, *International Journal of Forecasting* 9 (4) (1993) 527–529. doi:10.1016/0169-2070(93)90079-3.

- [50] F. X. Diebold, R. S. Mariano, Comparing predictive accuracy, *Journal of Business & Economic Statistics* 13 (3) (1995) 253–263. doi:10.1080/07350015.1995.10524599.
- [51] X. Glorot, Y. Bengio, Understanding the difficulty of training deep feedforward neural networks, in: *Proceedings of the International Conference on Artificial Intelligence and Statistics (AISTATS'10)*. Society for Artificial Intelligence and Statistics, 2010, pp. 249–256.
- [52] D. P. Kingma, J. Ba, Adam: A method for stochastic optimization, arXiv eprint (2014). arXiv:1412.6980.
- [53] Y. Yao, L. Rosasco, A. Caponnetto, On early stopping in gradient descent learning, *Constructive Approximation* 26 (2) (2007) 289–315. doi:10.1007/s00365-006-0663-2.
- [54] V. Nair, G. E. Hinton, Rectified linear units improve restricted boltzmann machines, in: *Proceedings of the 27th international Conference on Machine Learning (ICML)*, 2010, pp. 807–814, <http://icml2010.haifa.il.ibm.com/papers/432.pdf>.
- [55] J. Yosinski, J. Clune, Y. Bengio, H. Lipson, How transferable are features in deep neural networks?, in: Z. Ghahramani, M. Welling, C. Cortes, N. D. Lawrence, K. Q. Weinberger (Eds.), *Advances in Neural Information Processing Systems 27*, Curran Associates, Inc., 2014, pp. 3320–3328, <https://papers.nips.cc/paper/5347-how-transferable-are-features-in-deep-neural-networks>.
- [56] M. Jaderberg, V. Mnih, W. M. Czarnecki, T. Schaul, J. Z. Leibo, D. Silver, K. Kavukcuoglu, Reinforcement learning with unsupervised auxiliary tasks, arXiv eprint (2016). arXiv:1611.05397.
- [57] H. Nam, B. Han, Learning multi-domain convolutional neural networks for visual tracking, in: *Proceedings of the IEEE Conference on Computer Vision and Pattern Recognition*, 2016, pp. 4293–4302. doi:10.1109/CVPR.2016.465.
- [58] X. Li, L. Zhao, L. Wei, M.-H. Yang, F. Wu, Y. Zhuang, H. Ling, J. Wang, DeepSaliency: Multi-Task Deep Neural Network model for salient object detection, *IEEE Transactions on Image Processing* 25 (8) (2016) 3919–3930. doi:10.1109/TIP.2016.2579306.
- [59] F. E. Benth, J. S. Benth, S. Koekebakker, *Stochastic modelling of electricity and related markets*, Vol. 11, World Scientific, 2008. doi:10.1142/9789812812315.
- [60] H. He, E. A. Garcia, Learning from imbalanced data, *IEEE Transactions on Knowledge and Data Engineering* 21 (9) (2009) 1263–1284. doi:10.1109/TKDE.2008.239.
- [61] F. Chollet, Keras, <https://github.com/fchollet/keras> (2015).
- [62] Theano Development Team, Theano: A Python framework for fast computation of mathematical expressions, arXiv eprint (2016). arXiv:1605.02688.
- [63] RTE, Grid data, <https://data.rte-france.com/>. Accessed on 15.05.2017.
- [64] Elia, Grid data, <http://www.elia.be/en/grid-data/dashboard>. Accessed on 15.05.2017.
- [65] ENTSO-E transparency platform, <https://transparency.entsoe.eu/>. Accessed on 15.05.2017.
- [66] J. Bergstra, D. Yamins, D. D. Cox, Making a science of model search: Hyperparameter optimization in hundreds of dimensions for vision architectures, in: *Proceedings of the 30th International Conference on Machine Learning*, 2013, pp. 115–123, <http://proceedings.mlr.press/v28/bergstra13.pdf>.
- [67] J. Nowotarski, E. Raviv, S. Trück, R. Weron, An empirical comparison of alternative schemes for combining electricity spot price forecasts, *Energy Economics* 46 (2014) 395–412. doi:10.1016/j.eneco.2014.07.014.
- [68] R. Weron, A. Misiorek, Forecasting spot electricity prices with time series models, in: *Proceedings of the European Electricity Market EEM-05 Conference*, 2005, pp. 133–141.